

Journal Pre-proofs

Design, synthesis and evaluation of phthalide alkyl tertiary amine derivatives as promising acetylcholinesterase inhibitors with high potency and selectivity against Alzheimer's disease

Li Luo, Qing Song, Yan Li, Zhongcheng Cao, Xiaoming Qiang, Zhenghuai Tan, Yong Deng

PII: S0968-0896(20)30205-4
DOI: <https://doi.org/10.1016/j.bmc.2020.115400>
Reference: BMC 115400

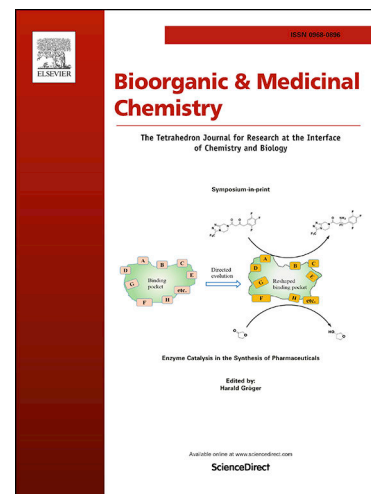
To appear in: *Bioorganic & Medicinal Chemistry*

Received Date: 7 January 2020
Revised Date: 17 February 2020
Accepted Date: 21 February 2020

Please cite this article as: L. Luo, Q. Song, Y. Li, Z. Cao, X. Qiang, Z. Tan, Y. Deng, Design, synthesis and evaluation of phthalide alkyl tertiary amine derivatives as promising acetylcholinesterase inhibitors with high potency and selectivity against Alzheimer's disease, *Bioorganic & Medicinal Chemistry* (2020), doi: <https://doi.org/10.1016/j.bmc.2020.115400>

This is a PDF file of an article that has undergone enhancements after acceptance, such as the addition of a cover page and metadata, and formatting for readability, but it is not yet the definitive version of record. This version will undergo additional copyediting, typesetting and review before it is published in its final form, but we are providing this version to give early visibility of the article. Please note that, during the production process, errors may be discovered which could affect the content, and all legal disclaimers that apply to the journal pertain.

© 2020 Elsevier Ltd. All rights reserved.



Design, synthesis and evaluation of phthalide alkyl tertiary amine derivatives as promising acetylcholinesterase inhibitors with high potency and selectivity against Alzheimer's disease

Li Luo^{a,b}, Qing Song^a, Yan Li^a, Zhongcheng Cao^a, Xiaoming Qiang^a, Zhenghuai Tan^c, Yong Deng^{a,*}

^aDepartment of Medicinal Chemistry, Key Laboratory of Drug-Targeting and Drug Delivery System of the Education Ministry and Sichuan Province, Sichuan Engineering Laboratory for Plant-Sourced Drug and Sichuan Research Center for Drug Precision Industrial Technology, West China School of Pharmacy, Sichuan University, Chengdu 611041, China

^bPrecision Pharmacy & Drug Development Center, Department of Pharmacy, Tangdu Hospital, Fourth Military Medical University, Xi'an, 710038, China

^cInstitute of Traditional Chinese Medicine Pharmacology and Toxicology, Sichuan academy of Chinese Medicine Sciences, Chengdu, 610041, P. R. China

**Corresponding Author.*

E-mail: dengyong@scu.edu.cn (Yong Deng)

Abstract

A series of phthalide alkyl tertiary amine derivatives were designed, synthesized and evaluated as potential multi-target agents against Alzheimer's disease (AD). The results indicated that almost all the compounds displayed significant AChE inhibitory and selective activities. Besides, most of the derivatives exhibited increased self-induced $A\beta_{1-42}$ aggregation inhibitory activity compared to the lead compound *DL*-NBP, and some compounds also exerted good antioxidant activity. Specifically, compound **I-8** showed the highest inhibitory potency toward AChE ($IC_{50} = 2.66$ nM), which was significantly better than Donepezil ($IC_{50} = 26.4$ nM). Moreover, molecular docking studies revealed that compound **I-8** could bind to both the catalytic active site and peripheral anionic site of AChE. Furthermore, compound **I-8** displayed excellent BBB permeability *in vitro*. Importantly, the step-down passive avoidance test indicated that **I-8** significantly reversed scopolamine-induced memory deficit in mice. Collectively, these results suggested that **I-8** might be a potent and selective AChE inhibitor for further anti-AD drug development.

Keywords: Alzheimer's disease; *DL*-3-*n*-butylphthalide derivatives; Multi-target agents; Acetylcholinesterase inhibitors; Anti- $A\beta$ aggregation; Antioxidant.

1. Introduction

Alzheimer's disease (AD), characterized by memory loss, language and cognitive impairment, and severe behavioral abnormalities, is an age-related and progressive neurodegenerative disorder. To date, an estimated 46 million people worldwide suffer from dementia, which is expected to reach 131.5 million by 2050.¹ Due to the complex and unidentified etiology, many factors are thought to be related to the occurrence and development of AD, including acetylcholine (ACh) declines, β -amyloid ($A\beta$) deposits, dyshomeostasis of biometals, oxidative stress and hyperphosphorylated τ -protein.^{2,3} Current clinical drugs for AD treatment can only temporarily and modestly improve the cognitive function, but can't significantly modify the course and the final outcome of the disease. Thus, there is an urgent need for new AD therapy strategies.

According to cholinergic hypothesis, the decline levels of ACh in specific regions of the brain leads to cognitive and memory impairments of AD.⁴ Acetylcholinesterase (AChE) and butyrylcholinesterase (BuChE) are the two types of cholinesterases to hydrolyze ACh in the central nervous system (CNS), and AChE has a 10 fold hydrolytic ACh activity than BuChE.^{4,5} Thus, selective inhibition of AChE is effective in AD therapy and beneficial to diminish peripheral cholinergic side effects of BuChE inhibitor.⁵ Moreover, it has been known that AChE contains catalytic active site (CAS) and peripheral anionic site (PAS), and the PAS contributes to aggregation of amyloid fibrils, obtaining stable AChE- $A\beta$ complexes, which are more toxic than single $A\beta$ peptide.⁶ Therefore, effective dual-site AChE inhibitors may be more valuable for the research of anti-AD drugs.

Another predominant hypothesis reveals that $A\beta$ peptides in the brain plays a key role in AD pathogenesis.⁷ The aggregation of $A\beta$ peptides, particularly $A\beta_{1-42}$, a key subtype with higher neuronal toxicity and accumulation rate than $A\beta_{1-40}$, initiates the pathogenic cascade and ultimately leads to neuronal dysfunction and dementia.⁷ Additionally, the progressive accumulation of $A\beta$ is accompanied by inflammation and oxidative stress, which further leads to neurodegeneration.⁸ As a result, prevention of $A\beta_{1-42}$ aggregation could serve as a rational strategy for AD treatment.

Besides, recent evidences demonstrated that oxidative stress is a central event in AD pathology, and associated with the formation and accumulation of both $A\beta$ plaques and neurofibrillary tangles.⁹ Moreover, the biochemical activity of Monoamine oxidases (MAOs) have been shown to produce hydrogen peroxide and cause oxidative stress.¹⁰ Currently, selective MAO-A inhibitors can improve depressive symptoms, while selective MAO-B inhibitors are beneficial for the treatment of

neurodegenerative disorders like AD.¹¹ Actually, AD patients commonly have depressive symptoms which have been considered as risk factors for the development of AD.¹² Thus, inhibition of MAOs and oxidative damage can be nominated as helpful therapeutics.

Therefore, because of the multiple and complex pathogenesis of AD, molecules aimed at a single target may be incapable of effectively altering the progression of the disease. In contrast, multifunctional molecules with two or more complementary biological activities may exert significant advantages against AD.¹³ Consequently, design of multi-target-directed ligands (MTDLs) which act on multiple pathophysiological pathways of AD has recently gained special attention and might represent an important advance in the treatment of AD.

DL-3-*n*-butylphthalide (**Figure 1**, *DL*-NBP) was approved for stroke treatment by the State Food and Drug Administration of China. Studies in stroke animal models have revealed that *DL*-NBP could increase the brain microcirculation, attenuate inflammation, mitochondrial dysfunction, oxidative damage and apoptosis.¹⁴⁻¹⁶ Recently, *DL*-NBP has been shown to significantly improve cognitive function in rats injected with *Aβ* peptide as well as in a mouse AD model carrying mutations in the genes encoding amyloid precursor protein and presenilin 1.^{17,18} Moreover, *DL*-NBP could protect against cognitive impairment in vascular dementia.^{19,20} These findings suggested that *DL*-NBP may exert a therapeutic efficacy for AD by targeting multiple key pathways of the disease pathogenesis. Donepezil (Aricept®), a clinically effective AChE inhibitor to treat mild-to-moderate AD, can bind CAS and PAS of AChE respectively through the benzyl piperidine and indanone moieties.²¹ Interestingly, *DL*-NBP also has a structure similar to indanone backbone, and previous studies reported by our group have shown that the tertiary amine fragments, which are derived from the ring-opening of the benzyl piperidine group of Donepezil, are key requirement for adequate AChE inhibition.^{22,23} Therefore, according to the MTDLs strategy, we combined *DL*-NBP with appropriate secondary amines using different lengths of carbon spacers to design a series of novel phthalide alkyl tertiary amines derivatives (**Figure 1**). In this study, all designed compounds were synthesized and evaluated for their biological activities, including AChE and BuChE, MAOs and *Aβ* aggregation inhibitory activities, as well as antioxidant effects. Besides, the outstanding compounds were selected for further evaluation of the ability to cross the blood-brain barrier (BBB) *in vitro* and the learning and memory effect *in vivo* using mice model.

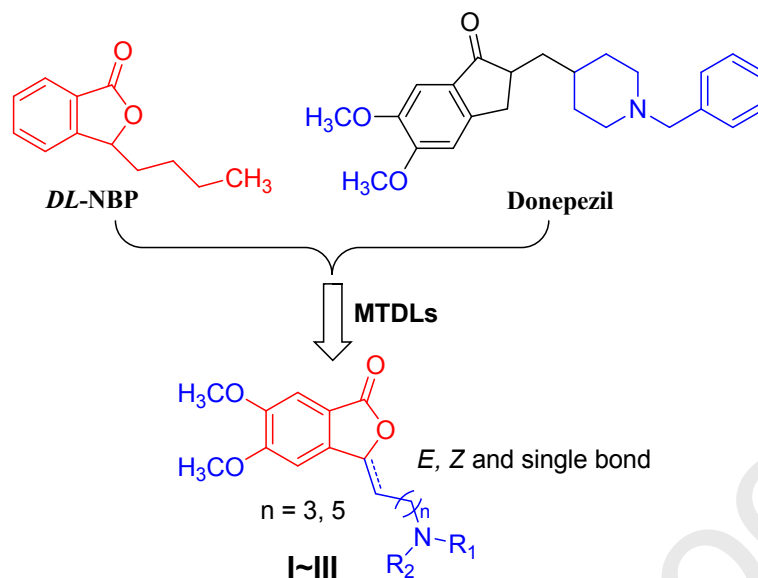


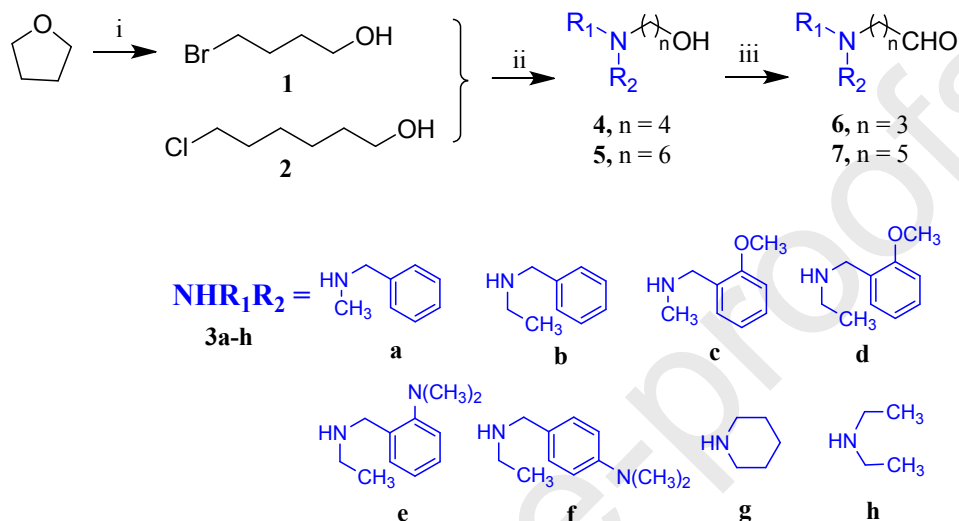
Figure 1. Design strategy for phthalide alkyl tertiary amines derivatives **I-III**.

2. Results and discussion

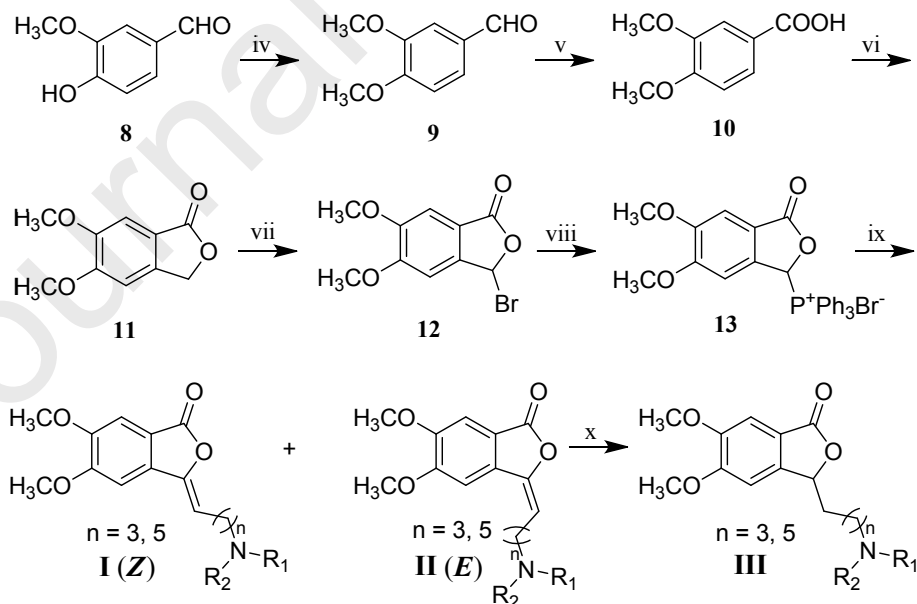
2.1. Chemistry

The synthetic routes for the target compounds were shown in **Scheme 1** and **Scheme 2**. 4-bromo-1-butanol (**1**) was prepared according to the literature using tetrahydrofuran as starting material.²⁴ Compounds **1** or 6-chloro-1-hexanol (**2**) were reacted with corresponding secondary amines **3a-h** in the presence of K_2CO_3 and DMF to afford the aminoalkyl alcohols **4** or **5**.²² Then, compound **4** or **5** reacted with $Py \cdot SO_3$ via the Parikh-Doering oxidation in the presence of dry DMSO and triethylamine to give the key intermediates aminoalkylaldehydes **6** or **7** respectively.²⁵ For the synthesis of target compounds phthalide alkyl tertiary amines **I-III**, vanillin (**8**) was used as starting material to obtain 3,4-dimethoxybenzoic acid (**10**) via methylation and oxidation respectively.²⁶ Then compound **10** reacted with 37 % formaldehyde and *conc.* HCl to give 5,6-dimethoxy-2-benzofuran-1(3*H*)-one (**11**),²⁷ and then brominated in chlorobenzene using *N*-bromosuccinimide and AIBN to obtain 3-bromo-5,6-dimethoxyisobenzofuran-1(3*H*)-one (**12**).^{28,29} This intermediate was substituted by triphenylphosphine to give Wittig reagent **13**.²⁹ Subsequently, compound **13** and corresponding aminoalkylaldehydes **6** or **7** were used to give the *Z*-isomer compounds **I** and *E*-isomer compounds **II** by Wittig reaction after separation by silica gel chromatography.³⁰ The stereochemistry of each isomer was elucidated on the basis of 1H NMR data and references.^{31,32} The protons at phthalide nucleus C_4 of the *E*-isomer are observed at lower field (for $CDCl_3$ solution: ca. 7.2 ppm cf. ca. 7.0 ppm for the *Z*-

isomer) because of the deshielding effect of the nearby alkyl group. Due to the deshielding effect caused by the influence of the ring oxygen, the vinyl proton in the *E*-isomer experiences a deshielding effect are observed at lower field than in the *Z*-isomer also. Finally, compounds **III** were obtained *via* the catalytic hydrogenation reduction. All derivatives were characterized by ^1H NMR, ^{13}C NMR and ESI-MS.



Scheme 1. Synthesis of aminoalkylaldehydes **6** and **7**. *Reagents and conditions:* (i) 40 % HBr aq., reflux (80%); (ii) NHR_1R_2 (**3a-h**), K_2CO_3 , DMF, r.t. (80~85%); (iii) $\text{Py}\cdot\text{SO}_3$, DMSO, CH_2Cl_2 , Et_3N , r.t. (63~70%).



Scheme 2. Synthesis of phthalide alkyl tertiary amines derivatives **I-III**. *Reagents and conditions:* (iv) Me_2SO_4 , K_2CO_3 , acetone, reflux (92%); (v) KMnO_4 , NaHCO_3 , H_2O , 90 °C (90%); (vi) 37 % HCHO aq., conc. HCl, 70 °C (43.5%); (vii) NBS, AIBN, PhCl, 85 °C (76%); (viii) PPh_3 , Toluene, reflux

(70%); (ix) **6** or **7**, CH₂Cl₂, Et₃N, r.t. (**I-1~9**: 14.2~20.2%; **II-1~10**: 21.0~30.6%); (x) 10% Pd/C, H₂, CH₃OH, r.t. (**III-1~10**: 58.7~85.6%).

2.2. Pharmacology

2.2.1. Inhibition of AChE and BuChE

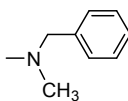
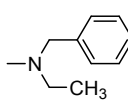
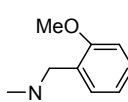
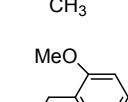
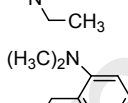
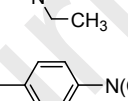
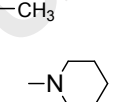
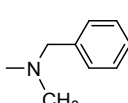
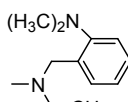
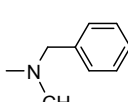
All synthesized derivatives were determined by modified Ellman's method for their inhibitory activities against AChE from *Electrophorus electricus* (EeAChE) and BuChE from rat serum (RatBuChE), using Donepezil as the reference drug.³³ As shown in **Table 1**, DL-NBP exhibited no inhibitory activity on AChE, while all target compounds showed good AChE inhibitory potency, implying that introduction of various carbon chain length tertiary amine moieties could significantly increase AChE inhibitory activity, which was consistent with our design strategy. Among them, compounds **I-8** and **II-9** displayed the most excellent efficiency to inhibit AChE (IC₅₀ = 2.66 and 4.84 nM, respectively), and both of which were stronger than Donepezil (IC₅₀ = 26.4 nM). In general, when the side chain length was the same (n = 3), compounds possessing an *N*-benzylmethylamine group usually displayed better AChE inhibitory activity than those with an *N*-benzylethylamine group (AChE inhibitory activity: **I-1** ≈ **I-2**, **II-1** > **II-2**, **III-1** > **III-2**). However, the adoption of 2-methoxy group to *N*-benzylmethylamine and *N*-benzylethylamine showed opposite regularity except **II-3** and **II-4** (AChE inhibitory activity: **I-3** ≈ **I-4**, **II-3** > **II-4**, **III-3** ≈ **III-4**). Moreover, the introduction of 2-dimethylamino group on the benzylamine moiety (**I-5**, **II-5** and **III-5**; IC₅₀ = 0.21, 0.35 and 0.26 μM, respectively) significantly improved AChE inhibitory potency, while the adoption of 4-dimethylamino group dramatically decreased the activity (**I-6**, **II-6** and **III-6**; IC₅₀ = 23.40, 13.80 and 24.90 μM, respectively). As a result, our results suggested that *N*-benzylmethylamine and *N*-(2-dimethylaminobenzyl) ethylamine might be more beneficial for AChE inhibition.

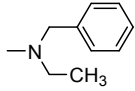
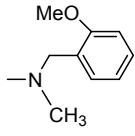
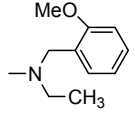
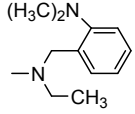
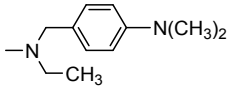
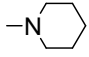
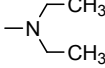
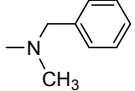
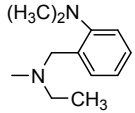
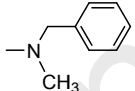
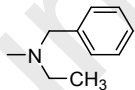
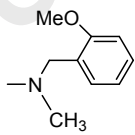
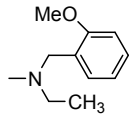
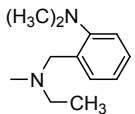
In order to study the effect of the linker length on the inhibition of AChE activity, *N*-benzylmethylamine and *N*-(2-dimethylaminobenzyl) ethylamine were fixed as tertiary amine structural units, and then compounds **I-8~9**, **II-9~10** and **III-9~10** were synthesized by increasing the length (n = 5). It revealed that the potency of the derivatives to inhibit AChE was enhanced with the carbon chain length increased (except **II-10** and **III-10**). For example, compounds **I-8**, **II-9** and **III-9** (n = 5) were much more potent than compounds **I-III-1** (n = 3). Compared with **I-8** (IC₅₀ = 0.00266 μM), the AChE inhibitory activity of **I-1** (IC₅₀ = 0.34 μM) was about 128-fold lower, and **II-1** (IC₅₀ = 0.64 μM)

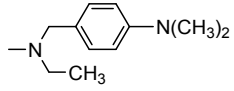
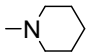
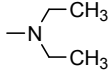
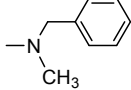
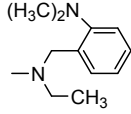
was almost 132-fold lower than that of **II-9** ($IC_{50} = 0.00484 \mu\text{M}$). Thus, the different linker of length was an important factor to inhibit AChE.

However, almost all compounds showed weak activity against BuChE, suggesting that these derivatives were potent AChE inhibitors with high selectivity toward AChE. The selectivity profile may be a limitation, but it was beneficial to diminish peripheral cholinergic side effects. For instance, tacrine, had severe side effects due to its poor selectivity to AChE.⁵

Table 1. Inhibition of *Ee*AChE and *Rat*BuChE activities, and oxygen radical absorbance capacity (ORAC, Trolox equivalents) by compounds **I-III**, *DL*-NBP and Donepezil.

Compound	NR_1R_2	n	$IC_{50} (\mu\text{M})^a$ <i>Ee</i> AChE	% Inhibition ^b <i>Rat</i> BuChE	ORAC ^c
I-1		3	0.34 ± 0.03	12.20 ± 0.25	0.32 ± 0.02
I-2		3	0.36 ± 0.02	17.30 ± 0.38	0.36 ± 0.03
I-3		3	1.64 ± 0.09	16.80 ± 0.46	0.44 ± 0.01
I-4		3	1.54 ± 0.07	18.70 ± 0.59	0.94 ± 0.05
I-5		3	0.21 ± 0.01	40.50 ± 0.94	0.78 ± 0.02
I-6		3	23.40 ± 0.98	13.60 ± 0.24	2.75 ± 0.08
I-7		3	4.56 ± 0.14	21.90 ± 0.83	0.28 ± 0.01
I-8		5	0.00266 ± 0.0001	19.10 ± 0.51	0.40 ± 0.02
I-9		5	0.0787 ± 0.002	38.08 ± 1.05	1.02 ± 0.05
II-1		3	0.64 ± 0.04	27.30 ± 0.64	0.49 ± 0.02

II-2		3	1.40 ± 0.06	11.00 ± 0.19	0.52 ± 0.03
II-3		3	0.41 ± 0.02	21.90 ± 0.47	0.38 ± 0.01
II-4		3	0.80 ± 0.06	19.10 ± 0.55	0.53 ± 0.03
II-5		3	0.35 ± 0.03	43.10 ± 0.83	1.07 ± 0.05
II-6		3	13.80 ± 0.29	14.10 ± 0.23	2.89 ± 0.08
II-7		3	0.44 ± 0.03	26.90 ± 0.54	0.32 ± 0.01
II-8		3	6.26 ± 0.34	4.19 ± 0.09	0.22 ± 0.01
II-9		5	0.00484 ± 0.0002	17.55 ± 0.63	0.43 ± 0.02
II-10		5	0.89 ± 0.05	35.20 ± 0.78	1.20 ± 0.06
III-1		3	0.35 ± 0.03	11.50 ± 0.21	0.29 ± 0.02
III-2		3	0.58 ± 0.04	23.10 ± 0.56	0.23 ± 0.01
III-3		3	0.49 ± 0.02	21.70 ± 0.39	0.27 ± 0.01
III-4		3	0.37 ± 0.02	29.80 ± 0.76	0.74 ± 0.04
III-5		3	0.26 ± 0.01	44.80 ± 0.91	0.43 ± 0.02

III-6		3	24.90 ± 0.91	6.20 ± 0.27	2.59 ± 0.07
III-7		3	15.80 ± 0.32	8.14 ± 0.19	0.22 ± 0.01
III-8		3	14.70 ± 0.48	5.10 ± 0.12	0.31 ± 0.02
III-9		5	0.16 ± 0.01	13.90 ± 0.23	0.25 ± 0.05
III-10		5	1.24 ± 0.03	40.45 ± 1.10	0.60 ± 0.04
<i>DL</i> -NBP	—	—	n.a. ^d	2.67 ± 0.06	0.21 ± 0.01
Donepezil	—	—	0.0264 ± 0.0010	IC ₅₀ = 44.6 ± 0.97 μM	NT ^e

^a AChE from *Electrophorus electricus*. IC₅₀ values represent the concentration of inhibitor required to decrease enzyme activity by 50% and are the mean of three independent experiments, each performed in triplicate. Data were expressed as mean ± SD (SD = standard deviation).

^b BuChE from rat serum. Tested compounds were used at 50 μM.

^c The mean ± SD of the three independent experiments. Data are expressed as μM of Trolox equivalent/μM of tested compound.

^d n.a. = no active. Compounds defined “no active” means a percent inhibition of less than 5.0% at a concentration of 50 μM in the assay conditions.

^e NT = not tested.

2.2.2. Docking study with AChE

In order to clarify the interacting modes between these derivatives and *Torpedo californica* (*Tc*) AChE (PDB: *IEVE*), a molecular modeling study was performed using the docking program, AutoDock 4.2 package with Discovery Studio 2.5.^{23,34} The most active compound **I-8** in AChE inhibition assay was chosen for our docking investigation. As shown in **Figure 2A**, compound **I-8** occupied the entire enzymatic CAS, the mid-gorge sites and PAS. One hydrogen bond was generated between the ligand **I-8** and the residue Phe288 (Phe288-NH•••O=**I-8**). The benzene ring of phthalein structure and benzylamine moiety in compound **I-8** could form π-π stacked interactions with Trp279 and Trp84, respectively. Moreover, the 3-substituted side chain folded in a conformation in the gorge that allowed it to interact with Tyr334, Phe330 and Phe331 *via* the hydrophobic interaction. These results indicated that **I-8** could stably bind to the CAS and PAS of AChE, which provided reasonably

explanation for its potent AChE inhibitory activity.

In addition, we also selected compounds **I-9**, **II-9** and **II-10** to investigate the interacting modes with AChE according to the results of AChE inhibition assay, to explore the effects of compounds with different configurations and substituents. **Figure 2B-D** revealed that compound **I-9** formed two hydrogen bonds with Phe288 and Arg 289 (Phe288-NH, Arg 289-NH •••O=**I-8**), while **II-9** and **II-10** both formed a hydrogen bond with Phe288, which was consistent with **I-8**. Likewise, the phthalein moiety in **I-9** and the benzylamine moiety in **II-9** and **II-10** could form π - π stacked interaction with Trp279 and Phe330, respectively. Moreover, hydrophobic interactions similar to **I-8** were also observed in compounds **I-9**, **II-9** and **II-10**. By and large, compounds that share the same structural framework act in the same way with AChE, occupying the CAS, the mid-gorge sites and PAS simultaneously.

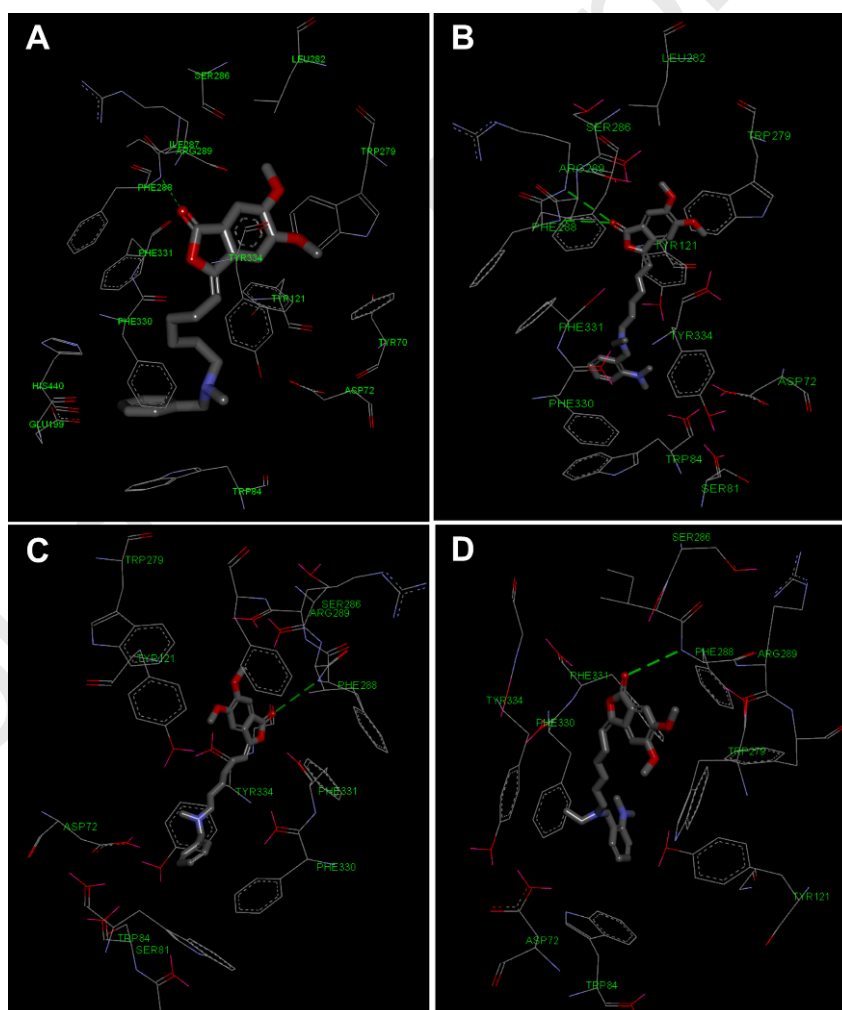


Figure 2. Docking pose of compounds **I-8** (A), **I-9** (B), **II-9** (C) and **II-10** (D) (colored by atom type) into the binding site of *TcAChE*, highlighting the protein residues that participate in the main

interactions with the inhibitor.

2.2.3. Evaluation for antioxidant activity

The antioxidant activity of these compounds was determined by the oxygen radical absorbance capacity of fluorescein (ORAC-FL) method.³⁵ Their ability to scavenge radicals (ORAC value) was provided as a Trolox (a vitamin E analog) equivalent, with their relative potency at 5 μ M compared with Trolox. The results from **Table 1** revealed that the antioxidant effect of all the target compounds was improved compared with *DL*-NBP (ORAC-FL value of 0.21 Trolox equivalent). Among them, **I-6**, **II-6** and **III-6** showed the most potent antioxidant activity with ORAC-FL values of 2.75, 2.89 and 2.59 Trolox equivalents, respectively, suggesting that the *N*-(4-dimethylaminobenzyl) ethylamine moiety seemed to be a potent substitution pattern to improve the antioxidant activity. However, other tertiary amine fragments and the length of the linker had no significant effect on their potency.

2.2.4. Inhibition of self-induced $A\beta_{1-42}$ aggregation and MAOs

All compounds were also tested by a thioflavin T fluorescence assay for their ability to inhibit self-induced $A\beta_{1-42}$ aggregation.^{36,37} Curcumin was used as the reference compound. Results summarized in **Table 2** indicated that the self-induced $A\beta_{1-42}$ aggregation inhibitory effect of these derivatives was better than that of the lead compound *DL*-NBP and Donepezil, but lower than curcumin (39.0%). According to the structure-activity relationship analysis, the potency of target derivatives to inhibit the self-aggregation of $A\beta_{1-42}$ slightly enhanced (except **III-10**) as the length of the alkyl chain increased, while the difference of tertiary amine group at the end of the side chain had no obvious regularity on its activity. On the whole, **III-1~10** displayed a slightly weaker inhibitory activity than **I-1~9** and **II-1~10**, indicating that the reduction of the double bond would destroy the large conjugated system of the compounds and reduce their inhibitory activity of self-induced $A\beta_{1-42}$ aggregation. Subsequently, we further tested human MAO-A and -B inhibitory activity of all the compounds.^{23,38} Clorgyline, Iproniazid and Rasagiline were used as reference compounds. Unfortunately, as shown in **Table 2**, these derivatives exhibited weak inhibitory activity against MAOs.

Table 2. Inhibition of MAOs and self-induced $A\beta_{1-42}$ aggregation activities by compounds **I-III**, *DL*-NBP and reference compounds.

Comp.	% inhibition ^{a,b}	self-induced $A\beta_{1-42}$
-------	-----------------------------	------------------------------

	MAO-A	MAO-B	aggregation
I-1	10.90 ± 0.23	11.90 ± 0.25	11.70 ± 0.12
I-2	10.40 ± 0.18	13.80 ± 0.32	17.00 ± 0.53
I-3	2.90 ± 0.02	10.30 ± 0.16	15.10 ± 0.31
I-4	26.70 ± 0.54	12.00 ± 0.29	23.80 ± 0.65
I-5	29.10 ± 0.38	9.90 ± 0.23	15.40 ± 0.22
I-6	12.90 ± 0.21	8.86 ± 0.17	22.00 ± 0.48
I-7	1.95 ± 0.08	32.30 ± 0.89	4.90 ± 0.08
I-8	7.9 ± 0.17	10.50 ± 0.20	19.45 ± 0.25
I-9	9.5 ± 0.12	14.70 ± 0.18	16.30 ± 0.32
II-1	17.90 ± 0.44	1.09 ± 0.03	8.60 ± 0.11
II-2	12.60 ± 0.18	15.80 ± 0.14	30.30 ± 0.73
II-3	4.90 ± 0.09	9.44 ± 0.12	19.10 ± 0.35
II-4	27.10 ± 0.56	4.80 ± 0.07	19.00 ± 0.73
II-5	30.00 ± 0.62	2.10 ± 0.09	8.20 ± 0.12
II-6	12.70 ± 0.27	17.00 ± 0.43	21.70 ± 0.48
II-7	1.52 ± 0.09	38.80 ± 0.85	11.30 ± 0.11
II-8	5.77 ± 0.24	19.70 ± 0.29	15.10 ± 0.41
II-9	22.30 ± 0.45	5.66 ± 0.09	12.36 ± 0.22
II-10	28.00 ± 0.70	7.30 ± 0.16	13.00 ± 0.19
III-1	8.00 ± 0.22	6.40 ± 0.24	8.90 ± 0.21
III-2	7.10 ± 0.15	5.51 ± 0.16	15.60 ± 0.35
III-3	0.25 ± 0.01	5.70 ± 0.30	14.40 ± 0.29
III-4	27.80 ± 0.42	10.40 ± 0.26	13.80 ± 0.14
III-5	17.80 ± 0.73	15.00 ± 0.50	15.30 ± 0.50
III-6	12.10 ± 0.24	9.47 ± 0.19	< 5.0
III-7	1.92 ± 0.07	34.70 ± 0.89	< 5.0
III-8	2.45 ± 0.05	21.50 ± 0.72	15.00 ± 0.36
III-9	7.88 ± 0.10	16.30 ± 0.35	12.98 ± 0.21
III-10	14.30 ± 0.25	13.45 ± 0.30	7.66 ± 0.19

<i>DL</i> -NBP	11.20 ± 0.17	18.20 ± 0.46	< 5.0
Curcumin	NT ^c	NT ^c	39.0 ± 1.3
Donepezil	NT ^c	NT ^c	< 5.0
Clorgyline	IC ₅₀ = 0.00791 ± 0.0002 μM	IC ₅₀ = 8.85 ± 0.201 μM	NT ^c
Rasagiline	IC ₅₀ = 0.712 ± 0.021 μM	IC ₅₀ = 0.0437 ± 0.002 μM	NT ^c
Iproniazid	IC ₅₀ = 1.37 ± 0.043 μM	IC ₅₀ = 4.32 ± 0.174 μM	NT ^c

^a Inhibition of MAOs and self-induced Aβ₁₋₄₂ aggregation by tested inhibitors at 10 μM and 25 μM respectively;

^b The mean ± SD of the three independent experiments;

^c NT = not tested.

2.2.5. Evaluation of drug-likeness properties

Based on above results, compounds **I-1**, **I-5**, **I-8**, **I-9**, **II~III-1**, **II~III-5**, **II~III-9** and **II~III-10** were selected to analyze their drug-likeness properties. Lipinski parameters, which describe the important molecular properties for drugs pharmacokinetics in the human body, especially their oral absorption, are calculated using online Molinspiration Property Calculator program.^{39,40} The rule requests that an oral active drug must not violate more than one of the following principles: MW < 500, log *P* < 5, hydrogen donors (nOHNH) < 5, hydrogen acceptors (nON) < 10. As shown in **Table 3**, the chosen compounds (except **III-10**) were in line with Lipinski's rule, suggesting that target compounds presented drug-likeness properties.

Table 3. Drug-likeness properties of selected compounds.

Compd.	MW ^a	log <i>P</i> ^b	tPSA ^c	nON ^d	nOHNH ^e	Volume ^f	nrotb ^g
I-1	367.44	3.23	51.92	5	0	347.64	8
I-5	424.54	3.66	55.16	6	0	410.35	10
I-8	395.50	4.24	51.92	5	0	381.24	10
I-9	452.60	4.67	55.16	6	0	443.95	12
II-1	367.44	3.23	51.92	5	0	347.64	8
II-5	424.54	3.66	55.16	6	0	410.35	10
II-9	395.50	4.24	51.92	5	0	381.24	10
II-10	452.60	4.67	55.16	6	0	443.95	12
III-1	369.46	3.64	48.01	5	0	353.85	9
III-5	426.56	4.07	51.25	6	0	416.56	11

III-9	397.51	4.65	48.01	5	0	387.45	11
III-10	454.61	5.08	51.25	6	0	450.16	13

^aMW: molecular weight; ^blog P: log octanol/water partition coefficient; ^ctPSA: total polar surface area; ^dnON: number of hydrogen acceptors; ^enOHNH: number of hydrogen donors; ^fVolume: molecular volume; ^gnrotb: number of rotatable bonds.

2.2.6. *In vitro* blood-brain barrier permeation assay

The permeability through blood-brain barrier (BBB) is an essential element for developing anti-AD drugs. To evaluate the *in vivo* BBB permeability of target derivatives, the parallel artificial membrane permeation assay of the blood-brain barrier (PAMPA-BBB) was employed.^{23,41} Compounds **I-8**, **II-9** and **III-9** were selected as representatives for BBB permeation assay. Eleven commercial drugs were chosen and evaluated for BBB permeability and compared with reported values to validate the assay (**Table S1**, Supplementary Material).⁴¹ A plot of experimental data versus the bibliographic values exhibited a good linear correlation: $P_e(\text{exp.}) = 0.8792 \times P_e(\text{bibl.}) - 0.0616$ ($R^2 = 0.9555$) (**Figure S1**, Supplementary Material). According to the correlation equation and the evaluation conditions established by Di *et al.*⁴¹, we defined that compounds with P_e values above 3.46×10^{-6} cm/s could pass through the BBB (**Table 4**). The results in **Table 5** indicated that compounds **I-8**, **II-9** and **III-9** could cross the BBB and reach their therapeutic targets in the CNS.

Table 4. Ranges of permeability of PAMPA-BBB assays ($P_e \times 10^{-6}$ cm/s).

High BBB permeation predicted (CNS +)	$P_e > 3.46$
Uncertain BBB permeation (CNS +/-)	$3.46 > P_e > 1.70$
Low BBB permeation predicted (CNS -)	$P_e < 1.70$

Table 5. Permeability results P_e ($\times 10^{-6}$ cm/s) from the PAMPA-BBB assay for selected compounds with their predicted penetration into the CNS.

Compd. ^a	P_e ($\times 10^{-6}$ cm/s) ^b	Prediction
I-8	10.06 ± 0.18	CNS +
II-9	10.31 ± 0.31	CNS +
III-9	13.58 ± 0.29	CNS +

^a Compounds were dissolved in DMSO at 5 mg/mL and diluted with PBS/EtOH (70:30). The final concentration of each compound was 100 μ g/mL.

^b Data are the mean \pm SD of three independent experiments.

2.2.7. Step-down passive avoidance test

Considering that good AChE inhibitory activity of these derivatives *in vitro*, we further investigated their effect on memory impairment induced by scopolamine in mice. The step-down passive avoidance test is extensively used to evaluate learning and memory in mice through the latency time in stepping down from the platform and the number of shocks, after an electric shock.^{22,42} The most active compound **I-8** in AChE inhibition assay was chosen for our test, with Donepezil as a positive control. As shown in **Figure 3**, compared with the control group, scopolamine-injected mice showed much shorter step-down latency time ($p < 0.01$), and the number of shocks was significantly increased ($p < 0.01$), which indicated the memory impairment. Treatment with compound **I-8** (1.0, 5.0 and 25.0 mg/kg) and Donepezil (5.0 mg/kg) obviously blocked these changes. Moreover, compared with Donepezil group, the medium dose group (5.0 mg/kg) showed longer latency time and fewer numbers of shocks, but the high dose (25.0 mg/kg) of compound **I-8** displayed a worse effect, suggesting that **I-8** may have some neurotoxicity. These results indicated that compound **I-8** could improve cognitive deficit by increasing brain cholinergic activity due to the inhibition of AChE.

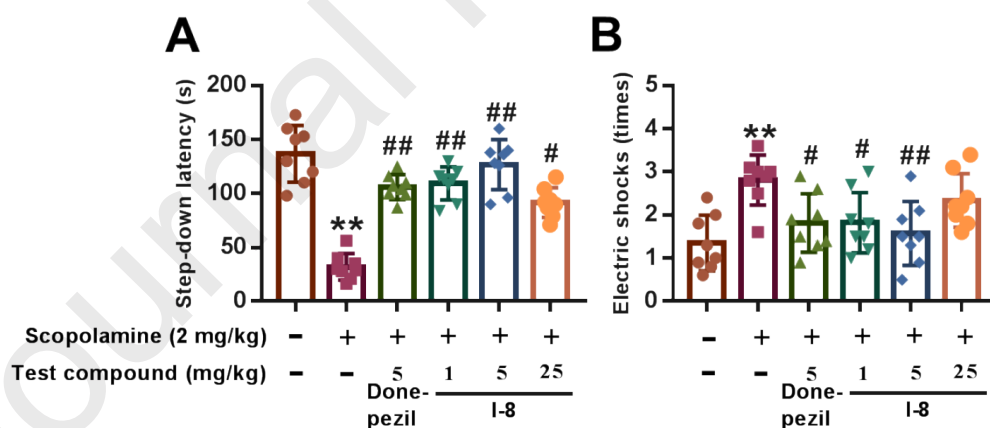


Figure 3. Effects of compound **I-8** on scopolamine-induced memory deficit in the step-down passive avoidance test. Compound **I-8** (1.0, 5.0, 25.0 mg/kg, *i.g.*) or Donepezil (5.0 mg/kg, *i.g.*) were given before scopolamine (2 mg/kg, *i.p.*) induced memory deficit. (A) latency time, (B) number of electric shocks. Values are expressed as the mean \pm SEM. $n = 8$ mice from three independent experiments; ** $p < 0.01$ versus control group; # $p < 0.05$, ## $p < 0.01$ versus scopolamine treated group.

3. Conclusion

In summary, almost all the phthalide alkyl tertiary amines derivatives exhibited significant inhibitory activity and selectivity of AChE. Among them, compound **I-8** displayed the most excellent activity on AChE with IC₅₀ value of 2.66 nM, which was significantly better than the control drug Donepezil. Furthermore, molecular docking studies showed that compound **I-8** could simultaneously bind to the CAS and PAS of AChE, and could penetrate the BBB. More interestingly, the *in vivo* study indicated that mice treated with **I-8** (5.0 mg/kg, *i.g.*) significantly reversed scopolamine- induced memory deficit, which was more effective than Donepezil (5.0 mg/kg, *i.g.*) in the step-down passive avoidance test. In addition, compared with the lead compound *DL*-NBP, these derivatives exhibited mild self-induced A β ₁₋₄₂ aggregation inhibitory activity, and some compounds also exerted good antioxidant activity. Therefore, most derivatives had potential multi-target anti-AD properties, among which compound **I-8** could be used as a highly effective and selective AChE inhibitor for the development of novel drugs in the treatment of AD.

4. Experimental section

4.1. Chemistry

All chemicals and solvents were purchased from commercial sources and used without further purification. Reactions were monitored by thin-layer chromatography (TLC) on silica gel GF₂₅₄ plates from Qingdao Haiyang Chemical Co. Ltd. (China), and the spots were detected under UV lamp (254 nm) or in iodine chamber. ¹H NMR and ¹³C NMR spectra were recorded on a Varian INOVA 400 NMR spectrometer or Varian INOVA 600 NMR spectrometer at room temperature using CDCl₃ or DMSO-*d*₆ as the solvent. Chemical shifts were expressed in parts per millions (ppm) using tetramethylsilane (TMS) as the internal standard. Coupling constants were reported in hertz. Column chromatography was accomplished on silica gel (230-400 mesh) purchased from Qingdao Haiyang Chemical Co. Ltd. (China). Melting points were determined on YRT-3 melting-point apparatus (China) and uncorrected. The purity of all compounds was measured by analytical reverse phase high-performance liquid chromatography (HPLC) with Shimadzu LC-10Avp plus system with a Kromasil C₁₈ column (4.6 mm×250 mm, 5 μ m). The mobile phase was a mixture of methanol and water at a flow rate of 1.0 mL/min. All target compounds possessed purity higher than 96%. MS spectra were performed on Agilent-627 TOF LC-MS Spectrometer.

4.1.1. Synthesis of 4-bromo-1-butanol (1)

40% HBr aqueous solution (35 mL) was added drop-wise to refluxing tetrahydrofuran (160 mL, 1.934 mol). Refluxing was then continued for 2 h. After cooling to room temperature, neutralised with saturated Na₂CO₃ aqueous solution and the resulting pale yellow organic layer was then separated. The aqueous layer was then extracted with dichloromethane (25 mL × 4). The combined organic phases were washed with brine, dried over sodium sulfate and filtered, concentrated under reduced pressure to obtain the crude product **1** as a yellow liquid, which was used without further purification.

4.1.2. General procedure for the synthesis of secondary amines (3a-f)

Compounds **3a-f** were prepared as previously described.⁴³

4.1.3. Synthesis of aminoalkyl alcohols (4 or 5)

Anhydrous K₂CO₃ (1.5 equiv.) and compounds **1** or **2** (1.5 equiv.) were added to a solution of the corresponding secondary amines **3a-h** (1.0 equiv.) in *N,N*-dimethylformamide (the synthesis of compound **5** required the addition of a catalytic amount of KI). The reaction mixture was stirred at room temperature overnight (the mixture was kept at 60 °C for the synthesis of compound **5**). Upon completion of the reaction, water was added to the mixture and then extracted with ethyl acetate. The combined organic phases were washed with 10% HCl aqueous solution. The acid aqueous layer was basified with 50% KOH aqueous solution to adjust the pH to 10 approximately and then extracted with dichloromethane. The combined organic phases were washed with water and brine, dried over anhydrous sodium sulfate and filtered, concentrated under reduced pressure to afford crude intermediates **4** or **5**.

4.1.4. Synthesis of aminoalkylaldehydes (6 or 7)

Dry dimethyl sulfoxide (20.0 equiv.) and triethylamine (5.0 equiv.) were added to a solution of compounds **4** or **5** (1.0 equiv.) in dry dichloromethane. When the mixture cooled to about -5°C by a freezing mixture of ice and salt, Py-SO₃ solid power (3.0 equiv.) was added slowly in portions. After the addition, the ice-salt bath was removed and the solution allowed to warm up to room temperature under an argon atmosphere for 1 h. The reaction mixture was basified with 10% NaOH aqueous solution and saturated NaHCO₃ solution to adjust the pH to 7-8. The aqueous phase was extracted with dichloromethane, then washed with brine, dried over sodium sulfate and filtered, concentrated under reduced pressure to give the crude compounds **6** or **7**.

4.1.5. Synthesis of 3,4-dimethoxybenzaldehyde (9)

To a mixture of compound **8** (15.0 g, 98.7 mmol) and anhydrous K_2CO_3 (20.5 g, 148.0 mmol) in acetone (200 mL), dimethyl sulfate (11.3 mL, 118.41 mmol) was added. The reaction mixture was refluxed for 3 h under an argon atmosphere. The mixture was filtered and the filtrate was concentrated to give compound **9**, which was used without further purification.

4.1.6. Synthesis of 3,4-dimethoxybenzoic acid (**10**)

Compound **9** (15.15 g, 91.17 mmol) and $NaHCO_3$ (9.19 g, 109.41 mmol) were suspended in H_2O (230 mL), then $KMnO_4$ (17.29 g, 109.41 mmol) was added slowly in an ice-water bath. The mixture was heated to 90 °C for 4 h. After the reaction mixture was cooled, filtered and the filtrate was acidified to pH = 3 by adding *conc.* HCl. The precipitate was filtered, washed with water and dried at room temperature to afford compound **10** as white solid.

4.1.7. Synthesis of 5,6-dimethoxy-2-benzofuran-1(3*H*)-one (**11**)

37% HCHO aqueous solution (60 mL) was added to a solution of compound **10** (14.58 g, 80.06 mmol) in *conc.* HCl (250 mL). The reaction mixture was heated at 70 °C for 8 h. After the mixture was cooled, filtered and the filtrate was extracted with dichloromethane (70 mL × 4). The combined organic phases were washed with saturated $NaHCO_3$ solution, water and brine orderly, dried over anhydrous sodium sulfate and filtered, concentrated under reduced pressure to afford the crude compound. The residue was recrystallized from ethanol to give compound **11** as a light brown solid, yield 43.5% (6.762 g), mp 151.5-153.8 °C (Lit.⁴⁴ 154-155 °C).

4.1.8. Synthesis of 3-bromo-5,6-dimethoxyisobenzofuran-1(3*H*)-one (**12**)

A mixture of compound **11** (6.76 g, 34.82 mmol) and AIBN (570 mg, 3.48 mmol) in dry chlorobenzene (100 mL) was heated to 85 °C under an argon atmosphere, then NBS (6.82 g, 38.31 mmol) was added slowly in portions. After the addition, the mixture was kept at 85 °C for 6 h. After cooling to room temperature, filtered and washed with dry chlorobenzene three times, concentrated under reduced pressure to give the crude compound **12**.

4.1.9. Synthesis of 5,6-dimethoxy-3-triphenyl phosphonium bromide phthalide (**13**)

Compound **12** (9.51 g, crude product) and triphenylphosphine (10.96 g, 41.79 mmol) were suspended in dry toluene (100 mL) and refluxed for 15 h under an argon atmosphere. The mixture was cooled to room temperature, filtered and washed with dry toluene three times. The filter cake was stirred in acetone uniformly and then filtered, washed with acetone and dried to afford compound **13**.

4.1.10. General procedure for the synthesis of butyphthalide tertiary amines derivatives (I-III)

A solution of compounds **6** or **7** (1.0 equiv.) and **13** (1.1 equiv.) in dry dichloromethane was stirred and cooled in an ice bath while dry triethylamine (1.1 equiv.) was added slowly dropwise. Stirring was continued at room temperature overnight under an argon atmosphere. The solvent was removed, then 10% HCl aqueous solution was added to adjust the pH to 1 and stirred for 5 min. The solution was washed with ethyl acetate and the aqueous layer was separated. The combined organic phases were washed with 10% HCl aqueous solution twice, then the combined acid aqueous layers were basified with 20% KOH aqueous solution and saturated NaHCO₃ solution to adjust the pH to 8. The aqueous phase was extracted with dichloromethane, then washed with brine, dried over anhydrous sodium sulfate and then concentrated at reduced pressure. The resultant yellow oil was purified *via* silica gel chromatography to give *Z*-isomer compounds **I-1~9** and *E*-isomer compounds **II-1~10**, respectively. Subsequently, a *E/Z* mixture of compounds **I** and **II** (1.0 equiv) in methanol (3 mL) and 10% Pd/C (0.2 equiv) was stirred under hydrogen (balloon) overnight. The mixture was filtered and the filtrate was concentrated to obtain crude compound. The residue was purified by silica gel chromatography to afford the desired products **III-1~10**.

(Z)-3-(4-(benzyl(methyl)amino)butylidene)-5,6-dimethoxyisobenzofuran-1(3H)-one(I-1)

It was synthesized from **13** and **6a** according to the general procedure, and then purified on silica gel chromatography eluted with dichloromethane/methanol (40:1) to obtain the pure product **I-1**. 15.8% yield; yellow oil. Purity: 98.8%. ¹H NMR (400 MHz, CDCl₃) δ 7.35-7.27 (m, 4H), 7.26-7.24 (m, 2H), 6.96 (s, 1H), 5.46 (t, *J* = 7.6 Hz, 1H), 4.00 (s, 3H), 3.95 (s, 3H), 3.55 (s, 2H), 2.50 (q, *J* = 7.6 Hz, 2H), 2.49 (t, *J* = 7.6 Hz, 2H), 2.21 (s, 3H), 1.81-1.75 (m, 2H); ¹³C NMR (100 MHz, CDCl₃) δ 167.2, 155.1, 151.1, 145.7, 138.3, 134.1, 129.1 (2C), 128.2 (2C), 127.0, 116.9, 107.4, 105.2, 100.7, 62.2, 56.4, 56.3 (2C), 41.9, 26.8, 23.5. HR-ESI-MS: Calcd. for C₂₂H₂₆NO₄ [M+H]⁺: 368.1862, found: 368.1865.

(Z)-3-(4-(benzyl(ethyl)amino)butylidene)-5,6-dimethoxyisobenzofuran-1(3H)-one (I-2)

It was synthesized from **13** and **6b** according to the general procedure, and then purified on silica gel chromatography eluted with dichloromethane/methanol (40:1) to obtain the pure product **I-2**. 14.2% yield; yellow oil. Purity: 98.9%. ¹H NMR (400 MHz, CDCl₃) δ 7.37 (d, *J* = 7.2 Hz, 2H), 7.32-7.27 (m, 2H), 7.24-7.21 (m, 2H), 6.94 (s, 1H), 5.42 (t, *J* = 7.6 Hz, 1H), 4.00 (s, 3H), 3.95 (s, 3H), 3.63 (s, 2H), 2.59-2.50 (m, 4H), 2.45 (q, *J* = 6.8 Hz, 2H), 1.75-1.72 (m, 2H), 1.09 (t, *J* = 6.8 Hz, 3H); ¹³C NMR (100 MHz, CDCl₃) δ 167.2, 155.0, 151.1, 145.5, 138.9, 134.1, 129.0 (2C), 128.4 (2C), 126.9, 116.8,

107.5, 105.1, 100.6, 57.8, 56.3, 56.2, 52.2, 47.1, 26.5, 23.5, 11.4. HR-ESI-MS: Calcd. for $C_{23}H_{28}NO_4$ $[M+H]^+$: 382.2018, found: 382.2016.

(Z)-5,6-dimethoxy-3-(4-((2-methoxybenzyl)(methyl)amino)butylidene)isobenzofuran-1(3H)-one (I-3)

It was synthesized from **13** and **6c** according to the general procedure, and then purified on silica gel chromatography eluted with petroleum ether/acetone (2:1) to obtain the pure product **I-3**. 18.5% yield; yellow oil. Purity: 99.2%. 1H NMR (400 MHz, $CDCl_3$) δ 7.37 (d, $J = 7.2$ Hz, 1H), 7.26 (t, $J = 7.2$ Hz, 1H), 7.24 (s, 1H), 6.99 (s, 1H), 6.92 (t, $J = 7.2$ Hz, 1H), 6.87 (d, $J = 7.2$ Hz, 1H), 5.50 (t, $J = 8.0$ Hz, 1H), 4.01 (s, 3H), 3.95 (s, 3H), 3.83 (s, 3H), 3.67 (s, 2H), 2.59 (t, $J = 7.2$ Hz, 2H), 2.49 (q, $J = 8.0$ Hz, 2H), 2.32 (s, 3H), 1.89-1.83 (m, 2H). HR-ESI-MS: Calcd. for $C_{23}H_{28}NO_5$ $[M+H]^+$: 398.1967, found: 398.1963.

(Z)-5,6-dimethoxy-3-(4-((2-methoxybenzyl)(ethyl)amino)butylidene)isobenzofuran-1(3H)-one (I-4)

It was synthesized from **13** and **6d** according to the general procedure, and then purified on silica gel chromatography eluted with dichloromethane/methanol (20:1) to obtain the pure product **I-4**. 16.4% yield; yellow oil. Purity: 98.5%. 1H NMR (400 MHz, $CDCl_3$) δ 7.67 (d, $J = 7.6$ Hz, 1H), 7.33 (t, $J = 7.6$ Hz, 1H), 7.24 (s, 1H), 7.04 (s, 1H), 6.98 (t, $J = 7.6$ Hz, 1H), 6.89 (d, $J = 7.6$ Hz, 1H), 5.53 (t, $J = 8.0$ Hz, 1H), 4.24 (s, 2H), 4.03 (s, 3H), 3.96 (s, 3H), 3.86 (s, 3H), 3.07 (q, $J = 8.0$ Hz, 2H), 2.96 (t, $J = 6.8$ Hz, 2H), 2.48 (q, $J = 7.2$ Hz, 2H), 2.21-2.17 (m, 2H), 1.44 (t, $J = 7.2$ Hz, 3H); ^{13}C NMR (100 MHz, $CDCl_3$) δ 167.5, 158.0, 155.2, 151.4, 146.5, 133.8, 133.2, 131.4, 121.1, 117.1, 116.7, 110.8, 105.0, 104.9, 101.1, 56.5, 56.3, 55.4, 50.9, 49.8, 47.0, 23.5, 23.0, 8.8. HR-ESI-MS: Calcd. for $C_{24}H_{30}NO_5$ $[M+H]^+$: 412.2124, found: 412.2125.

(Z)-3-(4-((2-(dimethylamino)benzyl)(ethyl)amino)butylidene)-5,6-dimethoxyisobenzofuran-1(3H)-one (I-5)

It was synthesized from **13** and **6e** according to the general procedure, and then purified on silica gel chromatography eluted with dichloromethane/methanol (20:1) to obtain the pure product **I-5**. 19.6% yield; yellow oil. Purity: 98.9%. 1H NMR (400 MHz, $CDCl_3$) δ 7.94 (d, $J = 7.6$ Hz, 1H), 7.33-7.28 (m, 2H), 7.23 (s, 1H), 7.20-7.14 (m, 1H), 7.05 (s, 1H), 5.52 (t, $J = 8.0$ Hz, 1H), 4.31 (s, 2H), 4.03 (s, 3H), 3.96 (s, 3H), 3.04-2.98 (m, 4H), 2.64 (s, 6H), 2.46 (q, $J = 7.2$ Hz, 2H), 2.19-2.13 (m, 2H), 1.36 (t, $J = 7.2$ Hz, 3H). HR-ESI-MS: Calcd. for $C_{25}H_{33}N_2O_4$ $[M+H]^+$: 425.2440, found: 425.2443.

(Z)-3-(4-((4-(dimethylamino)benzyl)(ethyl)amino)butylidene)-5,6-dimethoxyisobenzofuran-1(3H)-one (I-6)

It was synthesized from **13** and **6f** according to the general procedure, and then purified on silica gel chromatography eluted with dichloromethane/methanol (20:1) to obtain the pure product **I-6**. 18.3% yield; yellow oil. Purity: 99.0%. ¹H NMR (400 MHz, CDCl₃) δ 7.24 (s, 1H), 7.22 (d, *J* = 8.4 Hz, 2H), 6.98 (s, 1H), 6.67 (d, *J* = 8.4 Hz, 2H), 5.48 (t, *J* = 7.6 Hz, 1H), 4.00 (s, 3H), 3.95 (s, 3H), 3.65 (s, 2H), 2.92 (s, 6H), 2.63-2.60 (m, 4H), 2.46 (q, *J* = 7.6 Hz, 2H), 1.87-1.78 (m, 2H), 1.14 (t, *J* = 6.4 Hz, 3H). HR-ESI-MS: Calcd. for C₂₅H₃₃N₂O₄ [M+H]⁺: 425.2440, found: 425.2442.

(Z)-5,6-dimethoxy-3-(4-(piperidin-1-yl)butylidene)isobenzofuran-1(3H)-one (I-7)

It was synthesized from **13** and **6g** according to the general procedure, and then purified on silica gel chromatography eluted with dichloromethane/methanol (20:1) to obtain the pure product **I-7**. 14.3% yield; yellow oil. Purity: 99.4%. ¹H NMR (400 MHz, CDCl₃) δ 7.24 (s, 1H), 7.02 (s, 1H), 5.52 (t, *J* = 7.6 Hz, 1H), 4.01 (s, 3H), 3.95 (s, 3H), 2.62-2.55 (m, 6H), 2.49 (q, *J* = 7.6 Hz, 2H), 1.92-1.85 (m, 2H), 1.75-1.72 (m, 4H), 1.55-1.50 (m, 2H). HR-ESI-MS: Calcd. for C₁₉H₂₆NO₄ [M+H]⁺: 332.1862, found: 332.1858.

(Z)-3-(6-(benzyl(methyl)amino)hexylidene)-5,6-dimethoxyisobenzofuran-1(3H)-one (I-8)

It was synthesized from **13** and **7a** according to the general procedure, and then purified on silica gel chromatography eluted with dichloromethane/methanol (40:1) to obtain the pure product **I-8**. 17.7% yield; yellow oil. Purity: 99.0%. ¹H NMR (400 MHz, CDCl₃) δ 7.38-7.24 (m, 6H), 7.02 (s, 1H), 5.49 (t, *J* = 7.6 Hz, 1H), 4.01 (s, 3H), 3.95 (s, 3H), 3.67 (s, 2H), 2.53 (t, *J* = 7.2 Hz, 2H), 2.46 (q, *J* = 7.6 Hz, 2H), 2.32 (s, 3H), 1.69-1.60 (m, 2H), 1.56-1.50 (m, 2H), 1.44-1.38 (m, 2H). HR-ESI-MS: Calcd. for C₂₄H₃₀NO₄ [M+H]⁺: 396.2175, found: 396.2174.

(Z)-3-(6-((2-(dimethylamino)benzyl)(ethyl)amino)hexylidene)-5,6-dimethoxyisobenzofuran-1(3H)-one (I-9)

It was synthesized from **13** and **7e** according to the general procedure, and then purified on silica gel chromatography eluted with dichloromethane/methanol (40:1) to obtain the pure product **I-9**. 20.2% yield; yellow oil. Purity: 98.0%. ¹H NMR (600 MHz, CDCl₃) δ 7.81 (d, *J* = 7.2 Hz, 1H), 7.28 (t, *J* = 7.2 Hz, 1H), 7.23 (s, 1H), 7.15 (d, *J* = 7.2 Hz, 1H), 7.12 (t, *J* = 7.2 Hz, 1H), 7.04 (s, 1H), 5.49 (t, *J* = 8.4 Hz, 1H), 4.01 (s, 3H), 3.94 (s, 3H), 2.82 (s, 2H), 2.76-2.71 (m, 2H), 2.65 (s, 6H), 2.43 (q, *J* = 7.2

Hz, 2H), 1.76-1.72 (m, 2H), 1.55-1.50 (m, 2H), 1.42-1.35 (m, 2H), 1.30-1.22 (m, 5H). HR-ESI-MS: Calcd. for $C_{27}H_{37}N_2O_4$ $[M+H]^+$: 453.2753, found: 453.2750.

(E)-3-(4-(benzyl(methyl)amino)butylidene)-5,6-dimethoxyisobenzofuran-1(3H)-one (II-1)

It was synthesized from **13** and **6a** according to the general procedure, and then purified on silica gel chromatography eluted with dichloromethane/methanol (40:1) to obtain the pure product **II-1**. 23.9% yield; yellow oil. Purity: 99.5%. 1H NMR (400 MHz, $CDCl_3$) δ 7.30 (s, 1H), 7.29-7.26 (m, 5H), 7.21 (s, 1H), 5.71 (t, $J = 8.4$ Hz, 1H), 3.97 (s, 3H), 3.90 (s, 3H), 3.57 (s, 2H), 2.60 (q, $J = 8.4$ Hz, 2H), 2.57-2.53 (m, 2H), 2.26 (s, 3H), 1.84 (t, $J = 7.2$ Hz, 2H). HR-ESI-MS: Calcd. for $C_{22}H_{26}NO_4$ $[M+H]^+$: 368.1862, found: 368.1865.

(E)-3-(4-(benzyl(ethyl)amino)butylidene)-5,6-dimethoxyisobenzofuran-1(3H)-one (II-2)

It was synthesized from **13** and **6b** according to the general procedure, and then purified on silica gel chromatography eluted with dichloromethane/methanol (40:1) to obtain the pure product **II-2**. 25.3% yield; yellow oil. Purity: 99.2%. 1H NMR (400 MHz, $CDCl_3$) δ 7.33-7.24 (m, 6H), 7.17 (s, 1H), 5.68 (t, $J = 8.0$ Hz, 1H), 3.97 (s, 3H), 3.92 (s, 3H), 3.64 (s, 2H), 2.60-2.54 (m, 6H), 1.83-1.79 (m, 2H), 1.09 (t, $J = 7.2$ Hz, 2H). HR-ESI-MS: Calcd. for $C_{23}H_{28}NO_4$ $[M+H]^+$: 382.2018, found: 382.2012.

(E)-5,6-dimethoxy-3-(4-((2-methoxybenzyl)(methyl)amino)butylidene)isobenzofuran-1(3H)-one (II-3)

It was synthesized from **13** and **6c** according to the general procedure, and then purified on silica gel chromatography eluted with petroleum ether/acetone (2:1) to obtain the pure product **II-3**. 26.4% yield; yellow oil. Purity: 98.6%. 1H NMR (400 MHz, $CDCl_3$) δ 7.31 (d, $J = 7.6$ Hz, 1H), 7.28 (s, 1H), 7.24 (s, 1H), 7.22 (t, $J = 7.6$ Hz, 1H), 6.89 (t, $J = 7.6$ Hz, 1H), 6.84 (d, $J = 7.6$ Hz, 1H), 5.73 (t, $J = 8.0$ Hz, 1H), 3.96 (s, 3H), 3.86 (s, 3H), 3.79 (s, 3H), 3.59 (s, 2H), 2.62 (q, $J = 8.0$ Hz, 2H), 2.56 (t, $J = 6.8$ Hz, 2H), 2.26 (s, 3H), 1.90-1.83 (m, 2H); ^{13}C NMR (100 MHz, $CDCl_3$) δ 167.2, 157.8, 154.7, 151.0, 145.8, 132.7, 130.9, 128.5, 120.2, 118.8, 111.7, 110.3, 106.1, 105.5, 104.3, 69.1, 56.4, 56.2, 55.2, 42.3, 41.9, 27.0, 23.7. HR-ESI-MS: Calcd. for $C_{23}H_{28}NO_5$ $[M+H]^+$: 398.1967, found: 398.1963.

(E)-5,6-dimethoxy-3-(4-((2-methoxybenzyl)(ethyl)amino)butylidene)isobenzofuran-1(3H)-one (II-4)

It was synthesized from **13** and **6d** according to the general procedure, and then purified on silica gel chromatography eluted with dichloromethane/methanol (20:1) to obtain the pure product **II-4**. 23.7% yield; yellow oil. Purity: 99.3%. 1H NMR (400 MHz, $CDCl_3$) δ 7.46 (d, $J = 7.6$ Hz, 1H), 7.29 (s, 1H),

7.25 (t, $J = 7.6$ Hz, 1H), 7.20 (s, 1H), 6.90 (t, $J = 7.6$ Hz, 1H), 6.84 (d, $J = 7.6$ Hz, 1H), 5.67 (t, $J = 8.0$ Hz, 1H), 3.97 (s, 3H), 3.93 (s, 3H), 3.78 (s, 5H), 2.78-2.70 (m, 4H), 2.62 (q, $J = 7.6$ Hz, 2H), 1.98-1.88 (m, 2H), 1.16 (t, $J = 7.6$ Hz, 3H). HR-ESI-MS: Calcd. for $C_{24}H_{30}NO_5$ $[M+H]^+$: 412.2124, found: 412.2125.

(E)-3-(4-((2-(dimethylamino)benzyl)(ethyl)amino)butylidene)-5,6-dimethoxyisobenzofuran-1(3H)-one (II-5)

It was synthesized from **13** and **6e** according to the general procedure, and then purified on silica gel chromatography eluted with dichloromethane/methanol (20:1) to obtain the pure product **II-5**. 30.6% yield; yellow oil. Purity: 99.0%. 1H NMR (400 MHz, $CDCl_3$) δ 7.60 (d, $J = 7.2$ Hz, 1H), 7.29 (s, 1H), 7.20 (t, $J = 7.2$ Hz, 1H), 7.17 (s, 1H), 7.08 (d, $J = 7.2$ Hz, 1H), 6.99 (t, $J = 7.2$ Hz, 1H), 5.69 (t, $J = 7.6$ Hz, 1H), 3.96 (s, 3H), 3.94 (s, 3H), 3.72 (s, 2H), 2.65 (s, 6H), 2.61-2.54 (m, 6H), 1.82-1.78 (m, 2H), 1.08 (t, $J = 7.6$ Hz, 3H); ^{13}C NMR (100 MHz, $CDCl_3$) δ 167.5, 154.7, 153.0, 151.0, 145.6, 138.6, 132.6, 130.0, 127.5, 123.0, 118.9, 118.8, 111.8, 105.6, 104.2, 56.3, 52.5, 52.4, 47.6, 45.1 (2C), 29.6, 27.0, 23.9, 11.4. HR-ESI-MS: Calcd. for $C_{25}H_{33}N_2O_4$ $[M+H]^+$: 425.2440, found: 425.2443.

(E)-3-(4-((4-(dimethylamino)benzyl)(ethyl)amino)butylidene)-5,6-dimethoxyisobenzofuran-1(3H)-one (II-6)

It was synthesized from **13** and **6f** according to the general procedure, and then purified on silica gel chromatography eluted with dichloromethane/methanol (20:1) to obtain the pure product **II-6**. 27.2% yield; yellow oil. Purity: 98.6%. 1H NMR (400 MHz, $CDCl_3$) δ 7.30 (s, 1H), 7.18 (s, 1H), 7.15 (d, $J = 8.4$ Hz, 2H), 6.64 (d, $J = 8.4$ Hz, 2H), 5.72 (t, $J = 8.0$ Hz, 1H), 3.96 (s, 3H), 3.91 (s, 3H), 3.50 (s, 2H), 2.92 (s, 6H), 2.58-2.54 (m, 6H), 1.78-1.75 (m, 2H), 1.04 (t, $J = 6.8$ Hz, 3H); ^{13}C NMR (100 MHz, $CDCl_3$) δ 167.1, 154.6, 150.8, 149.6, 145.5, 132.6, 129.7 (2C), 126.4, 118.7, 112.2 (2C), 111.9, 105.4, 104.2, 57.2, 56.2 (2C), 51.8, 46.9 (2C), 40.5, 27.0, 23.8, 11.4. HR-ESI-MS: Calcd. for $C_{25}H_{33}N_2O_4$ $[M+H]^+$: 425.2440, found: 425.2442.

(E)-5,6-dimethoxy-3-(4-(piperidin-1-yl)butylidene)isobenzofuran-1(3H)-one (II-7)

It was synthesized from **13** and **6g** according to the general procedure, and then purified on silica gel chromatography eluted with dichloromethane/methanol (20:1) to obtain the pure product **II-7**. 21.0% yield; yellow oil. Purity: 99.2%. 1H NMR (400 MHz, $CDCl_3$) δ 7.30 (s, 1H), 7.22 (s, 1H), 5.73 (t, $J = 8.0$ Hz, 1H), 4.03 (s, 3H), 3.97 (s, 3H), 2.59 (q, $J = 7.6$ Hz, 2H), 2.47 (t, $J = 7.2$ Hz, 6H), 1.87-1.80 (m, 2H), 1.64-1.60 (m, 4H), 1.48-1.45 (m, 2H); ^{13}C NMR (100 MHz, $CDCl_3$) δ 167.1, 154.7, 151.0, 145.7,

132.6, 118.9, 111.5, 105.6, 104.2, 58.3, 56.5, 56.3, 54.5 (2C), 26.5, 25.5 (2C), 24.1, 24.0. HR-ESI-MS: Calcd. for C₁₉H₂₆NO₄ [M+H]⁺: 332.1862, found: 332.1859.

(E)-3-(4-(diethylamino)butylidene)-5,6-dimethoxyisobenzofuran-1(3H)-one (II-8)

It was synthesized from **13** and **6h** according to the general procedure, and then purified on silica gel chromatography eluted with dichloromethane/methanol (20:1) to obtain the pure product **II-8**. 23.6% yield; yellow oil. Purity: 98.7%. ¹H NMR (600 MHz, CDCl₃) δ 7.30 (s, 1H), 7.25 (s, 1H), 5.72 (t, *J* = 7.2 Hz, 1H), 4.04 (s, 3H), 3.97 (s, 3H), 2.69-2.64 (m, 6H), 2.60 (q, *J* = 7.2 Hz, 2H), 1.85-1.82 (m, 2H), 1.09 (t, *J* = 7.2 Hz, 6H); ¹³C NMR (150 MHz, CDCl₃) δ 167.1, 154.8, 151.1, 145.9, 132.6, 118.9, 111.1, 105.6, 104.3, 56.5, 56.3, 51.9, 46.8 (2C), 26.6, 23.9 (2C), 10.9. HR-ESI-MS: Calcd. for C₁₈H₂₆NO₄ [M+H]⁺: 320.1862, found: 320.1866.

(E)-3-(6-(benzyl(methyl)amino)hexylidene)-5,6-dimethoxyisobenzofuran-1(3H)-one (II-9)

It was synthesized from **13** and **7a** according to the general procedure, and then purified on silica gel chromatography eluted with dichloromethane/methanol (40:1) to obtain the pure product **II-9**. 26.0% yield; yellow oil. Purity: 99.0%. ¹H NMR (400 MHz, CDCl₃) δ 7.32-7.23 (m, 6H), 7.16 (s, 1H), 5.74 (t, *J* = 8.0 Hz, 1H), 3.99 (s, 3H), 3.96 (s, 3H), 3.49 (s, 2H), 2.51 (q, *J* = 7.6 Hz, 2H), 2.39 (t, *J* = 7.2 Hz, 2H), 2.20 (s, 3H), 1.62-1.55 (m, 4H), 1.49-1.43 (m, 2H); ¹³C NMR (100 MHz, CDCl₃) δ 167.1, 154.7, 151.0, 145.5, 138.6, 132.6, 129.0 (2C), 128.1 (2C), 126.9, 118.9, 111.9, 105.6, 104.0, 62.2, 57.0, 56.3 (2C), 42.1, 29.5, 27.1, 26.9, 26.0. HR-ESI-MS: Calcd. for C₂₄H₃₀NO₄ [M+H]⁺: 396.2175, found: 396.2172.

(E)-3-(6-((2-(dimethylamino)benzyl)(ethyl)amino)hexylidene)-5,6-dimethoxyisobenzofuran-1(3H)-one (II-10)

It was synthesized from **13** and **7e** according to the general procedure, and then purified on silica gel chromatography eluted with dichloromethane/methanol (40:1) to obtain the pure product **II-10**. 30.5% yield; yellow oil. Purity: 98.4%. ¹H NMR (400 MHz, CDCl₃) δ 7.66 (d, *J* = 7.6 Hz, 1H), 7.30 (s, 1H), 7.23 (t, *J* = 7.6 Hz, 1H), 7.16 (s, 1H), 7.10 (d, *J* = 7.6 Hz, 1H), 7.06 (t, *J* = 7.6 Hz, 1H), 5.72 (t, *J* = 8.0 Hz, 1H), 4.00 (s, 3H), 3.96 (s, 3H), 3.78 (s, 2H), 2.66 (s, 6H), 2.64-2.48 (m, 6H), 1.63-1.55 (m, 4H), 1.46-1.38 (m, 2H), 1.11 (t, *J* = 7.6 Hz, 3H); ¹³C NMR (150 MHz, CDCl₃) δ 167.1, 154.7, 153.1, 151.0, 145.5, 138.6, 132.6, 130.4, 127.9, 123.4, 119.1, 118.8, 111.9, 105.6, 104.0, 56.4, 56.2, 52.8, 52.0, 47.3, 45.2 (2C), 29.3, 26.9, 26.0, 25.8, 10.9. HR-ESI-MS: Calcd. for C₂₇H₃₇N₂O₄ [M+H]⁺: 453.2753, found: 453.2751.

3-(4-(benzyl(methyl)amino)butyl)-5,6-dimethoxyisobenzofuran-1(3H)-one (III-1)

It was synthesized according to the general procedure, and then purified on silica gel chromatography eluted with dichloromethane/methanol (30:1) to obtain the pure product **III-1**. 78.1% yield; yellow oil. Purity: 99.4%. ¹H NMR (400 MHz, CDCl₃) δ 7.32-7.25 (m, 6H), 6.80 (s, 1H), 5.37 (dd, *J* = 3.6, 7.6 Hz, 1H), 3.97 (s, 3H), 3.94 (s, 3H), 3.52 (s, 2H), 2.41 (t, *J* = 6.8 Hz, 2H), 2.22 (s, 3H), 2.04-1.99 (m, 1H), 1.73-1.69 (m, 1H), 1.62-1.58 (m, 2H), 1.54-1.47 (m, 2H); ¹³C NMR (100 MHz, CDCl₃) δ 170.8, 154.7, 150.3, 144.4, 138.1, 129.1 (2C), 128.2 (2C), 127.1, 117.9, 105.9, 103.0, 80.6, 62.1, 56.6, 56.3, 56.2, 41.9, 34.5, 26.7, 22.4. HR-ESI-MS: Calcd. for C₂₂H₂₈NO₄ [M+H]⁺: 370.2018, found: 370.2015.

3-(4-(benzyl(ethyl)amino)butyl)-5,6-dimethoxyisobenzofuran-1(3H)-one (III-2)

It was synthesized according to the general procedure, and then purified on silica gel chromatography eluted with dichloromethane/methanol (30:1) to obtain the pure product **III-2**. 74.6% yield; yellow oil. Purity: 99.0%. ¹H NMR (400 MHz, CDCl₃) δ 7.42-7.27 (m, 6H), 6.81 (s, 1H), 5.36 (dd, *J* = 3.6, 8.0 Hz, 1H), 3.98 (s, 3H), 3.94 (s, 3H), 3.78 (s, 2H), 2.72-2.61 (m, 4H), 2.04-2.03 (m, 1H), 1.75-1.65 (m, 3H), 1.52-1.46 (m, 2H), 1.18 (t, *J* = 6.8 Hz, 3H); ¹³C NMR (100 MHz, CDCl₃) δ 170.9, 154.7, 150.4, 144.5, 138.8, 129.0 (2C), 128.2 (2C), 127.0, 117.9, 106.0, 103.1, 80.6, 57.8, 56.4, 56.3, 52.5, 47.2, 34.5, 26.4, 22.5, 11.3. HR-ESI-MS: Calcd. for C₂₃H₃₀NO₄ [M+H]⁺: 384.2175, found: 384.2176.

5,6-dimethoxy-3-(4-((2-methoxybenzyl)(methyl)amino)butyl)isobenzofuran-1(3H)-one (III-3)

It was synthesized according to the general procedure, and then purified on silica gel chromatography eluted with petroleum ether/acetone (2:1) to obtain the pure product **III-3**. 82.1% yield; yellow oil. Purity: 97.6%. ¹H NMR (400 MHz, CDCl₃) δ 7.34 (d, *J* = 7.6 Hz, 1H), 7.28 (s, 1H), 7.24 (t, *J* = 7.6 Hz, 1H), 6.93 (t, *J* = 7.6 Hz, 1H), 6.87 (d, *J* = 7.6 Hz, 1H), 6.82 (s, 1H), 5.37 (dd, *J* = 3.6, 7.6 Hz, 1H), 3.97 (s, 3H), 3.94 (s, 3H), 3.83 (s, 3H), 3.62 (s, 2H), 2.49 (t, *J* = 7.2 Hz, 2H), 2.29 (s, 3H), 2.07-2.02 (m, 1H), 1.76-1.66 (m, 3H), 1.56-1.48 (m, 2H); ¹³C NMR (100 MHz, CDCl₃) δ 170.9, 157.8, 154.7, 150.4, 144.5, 138.1, 131.0, 128.6, 120.3, 117.9, 110.4, 106.0, 103.1, 80.6, 56.9, 56.4, 56.2, 55.4, 55.1, 41.9, 34.6, 26.5, 22.6. HR-ESI-MS: Calcd. for C₂₃H₃₀NO₅ [M+H]⁺: 400.2124, found: 400.2127.

5,6-dimethoxy-3-(4-((2-methoxybenzyl)(ethyl)amino)butyl)isobenzofuran-1(3H)-one (III-4)

It was synthesized according to the general procedure, and then purified on silica gel chromatography eluted with petroleum ether/acetone (2:1) to obtain the pure product **III-4**. 75.8%

yield; yellow oil. Purity: 99.0%. ^1H NMR (400 MHz, CDCl_3) δ 7.44 (d, $J = 7.6$ Hz, 1H), 7.27 (s, 1H), 7.23 (t, $J = 7.6$ Hz, 1H), 6.94 (t, $J = 7.6$ Hz, 1H), 6.86 (d, $J = 7.6$ Hz, 1H), 6.81 (s, 1H), 5.35 (dd, $J = 3.6, 7.6$ Hz, 1H), 3.97 (s, 3H), 3.94 (s, 3H), 3.82 (s, 3H), 3.71 (s, 2H), 2.63 (q, $J = 6.8$ Hz, 2H), 2.55 (t, $J = 7.2$ Hz, 2H), 2.04-1.99 (m, 1H), 1.73-1.64 (m, 3H), 1.56-1.47 (m, 2H), 1.12 (t, $J = 6.8$ Hz, 3H); ^{13}C NMR (150 MHz, CDCl_3) δ 170.9, 157.7, 154.7, 150.4, 144.5, 138.1, 130.6, 128.4, 120.4, 117.9, 110.3, 106.0, 103.1, 80.6, 56.4, 56.2, 55.3, 52.7, 51.0, 47.5, 34.5, 26.1, 22.6, 11.2. HR-ESI-MS: Calcd. for $\text{C}_{24}\text{H}_{32}\text{NO}_5$ $[\text{M}+\text{H}]^+$: 414.2280, found: 414.2278.

3-(4-((2-(dimethylamino)benzyl)(ethyl)amino)butyl)-5,6-dimethoxyisobenzofuran-1(3H)-one (III-5)

It was synthesized according to the general procedure, and then purified on silica gel chromatography eluted with dichloromethane/methanol (20:1) to obtain the pure product **III-5**. 80.3% yield; yellow oil. Purity: 99.5%. ^1H NMR (400 MHz, CDCl_3) δ 7.65 (d, $J = 7.6$ Hz, 1H), 7.27 (s, 1H), 7.23 (t, $J = 7.6$ Hz, 1H), 7.10 (d, $J = 7.6$ Hz, 1H), 7.06 (t, $J = 7.6$ Hz, 1H), 6.81 (s, 1H), 5.35 (dd, $J = 3.6, 7.6$ Hz, 1H), 3.98 (s, 3H), 3.94 (s, 3H), 3.81 (s, 2H), 2.66 (s, 6H), 2.65-2.58 (m, 4H), 2.01-1.99 (m, 1H), 1.70-1.65 (m, 3H), 1.53-1.43 (m, 2H), 1.12 (t, $J = 6.8$ Hz, 3H); ^{13}C NMR (100 MHz, CDCl_3) δ 170.9, 154.8, 150.4, 144.5, 138.1, 130.6, 127.7, 123.4, 119.2, 117.9, 109.6, 106.0, 103.1, 80.6, 56.4, 56.2, 52.7, 52.0, 47.4, 45.3 (2C), 34.5, 26.0, 22.5, 11.2. HR-ESI-MS: Calcd. for $\text{C}_{25}\text{H}_{35}\text{N}_2\text{O}_4$ $[\text{M}+\text{H}]^+$: 427.2597, found: 427.2592.

3-(4-((4-(dimethylamino)benzyl)(ethyl)amino)butyl)-5,6-dimethoxyisobenzofuran-1(3H)-one (III-6)

It was synthesized according to the general procedure, and then purified on silica gel chromatography eluted with dichloromethane/methanol (20:1) to obtain the pure product **III-6**. 85.6% yield; yellow oil. Purity: 99.4%. ^1H NMR (400 MHz, CDCl_3) δ 7.28 (s, 1H), 7.18 (d, $J = 8.4$ Hz, 2H), 6.81 (s, 1H), 6.68 (d, $J = 8.4$ Hz, 2H), 5.35 (dd, $J = 3.6, 8.0$ Hz, 1H), 3.97 (s, 3H), 3.93 (s, 3H), 3.56 (s, 2H), 2.93 (s, 6H), 2.56 (q, $J = 6.8$ Hz, 2H), 2.47 (t, $J = 7.6$ Hz, 2H), 2.03-1.98 (m, 1H), 1.73-1.66 (m, 1H), 1.62-1.52 (m, 2H), 1.48-1.45 (m, 2H), 1.08 (t, $J = 6.8$ Hz, 3H); ^{13}C NMR (100 MHz, CDCl_3) δ 170.9, 154.7, 150.4, 149.8, 144.5, 130.1 (2C), 125.7, 117.9, 112.4 (2C), 106.0, 103.2, 80.6, 56.9, 56.3, 56.2, 52.1, 46.8, 40.6, 34.5, 26.1, 22.5 (2C), 11.1. HR-ESI-MS: Calcd. for $\text{C}_{25}\text{H}_{35}\text{N}_2\text{O}_4$ $[\text{M}+\text{H}]^+$: 427.2597, found: 427.2594.

3-(4-((4-(dimethylamino)benzyl)(ethyl)amino)butyl)-5,6-dimethoxyisobenzofuran-1(3H)-one (III-7)

It was synthesized according to the general procedure, and then purified on silica gel chromatography eluted with dichloromethane/methanol (20:1) to obtain the pure product **III-7**. 62.1% yield; yellow oil. Purity: 99.2%. ¹H NMR (400 MHz, CDCl₃) δ 7.26 (s, 1H), 6.89 (s, 1H), 5.40 (dd, *J* = 3.2, 8.0 Hz, 1H), 4.01 (s, 3H), 3.94 (s, 3H), 2.95-2.90 (m, 4H), 2.78 (t, *J* = 8.0 Hz, 2H), 2.20-2.12 (m, 1H), 1.95-1.88 (m, 6H), 1.80-1.71 (m, 1H), 1.61-1.45 (m, 4H); ¹³C NMR (100 MHz, CDCl₃) δ 170.8, 154.9, 150.5, 144.2, 117.7, 105.9, 103.2, 80.2, 57.5, 56.5, 56.2, 53.5 (2C), 34.0, 24.0, 23.2 (2C), 22.6, 22.2. HR-ESI-MS: Calcd. for C₁₉H₂₈NO₄ [M+H]⁺: 334.2018, found: 334.2023.

3-(4-(diethylamino)butyl)-5,6-dimethoxyisobenzofuran-1(3H)-one (III-8)

It was synthesized according to the general procedure, and then purified on silica gel chromatography eluted with dichloromethane/methanol (20:1) to obtain the pure product **III-8**. 67.4% yield; yellow oil. Purity: 99.3%. ¹H NMR (400 MHz, CDCl₃) δ 7.27 (s, 1H), 6.89 (s, 1H), 5.41 (dd, *J* = 3.2, 8.0 Hz, 1H), 4.01 (s, 3H), 3.94 (s, 3H), 3.12 (q, *J* = 7.2 Hz, 4H), 2.95 (t, *J* = 6.8 Hz, 2H), 2.24-2.15 (m, 1H), 2.01-1.93 (m, 2H), 1.80-1.72 (m, 1H), 1.61-1.48 (m, 2H), 1.40 (t, *J* = 7.2 Hz, 6H); ¹³C NMR (150 MHz, CDCl₃) δ 170.7, 155.0, 150.5, 144.0, 117.6, 106.0, 103.2, 80.0, 56.5, 56.3, 51.4, 46.3 (2C), 33.8, 23.4 (2C), 22.1, 8.4. HR-ESI-MS: Calcd. for C₁₈H₂₈NO₄ [M+H]⁺: 322.2018, found: 322.2015.

3-(6-(benzyl(methyl)amino)hexyl)-5,6-dimethoxyisobenzofuran-1(3H)-one (III-9)

It was synthesized according to the general procedure, and then purified on silica gel chromatography eluted with dichloromethane/methanol (40:1) to obtain the pure product **III-9**. 58.7% yield; yellow oil. Purity: 98.9%. ¹H NMR (600 MHz, CDCl₃) δ 7.32-7.25 (m, 6H), 6.82 (s, 1H), 5.36 (dd, *J* = 3.6, 8.4 Hz, 1H), 3.98 (s, 3H), 3.94 (s, 3H), 3.51 (s, 2H), 2.38 (t, *J* = 7.2 Hz, 2H), 2.20 (s, 3H), 2.03-1.99 (m, 1H), 1.72-1.69 (m, 1H), 1.55-1.50 (m, 2H), 1.49-1.43 (m, 2H), 1.39-1.33 (m, 4H); ¹³C NMR (100 MHz, CDCl₃) δ 170.8, 154.6, 150.3, 144.5, 138.5, 129.0 (2C), 128.1 (2C), 126.9, 117.9, 105.9, 103.0, 80.7, 62.1, 57.1, 56.3, 56.1, 41.9, 34.6, 29.1, 27.0, 26.9, 24.6. HR-ESI-MS: Calcd. for C₂₄H₃₂NO₄ [M+H]⁺: 398.2331, found: 398.2336.

3-(6-((2-(dimethylamino)benzyl)(ethyl)amino)hexyl)-5,6-dimethoxyisobenzofuran-1(3H)-one (III-10)

It was synthesized according to the general procedure, and then purified on silica gel chromatography eluted with dichloromethane/methanol (20:1) to obtain the pure product **III-10**. 63.5% yield; yellow oil. Purity: 98.5%. ¹H NMR (400 MHz, CDCl₃) δ 7.69 (d, *J* = 7.6 Hz, 1H), 7.28 (s, 1H),

7.24 (t, $J = 7.6$ Hz, 1H), 7.12 (d, $J = 7.6$ Hz, 1H), 7.08 (t, $J = 7.6$ Hz, 1H), 6.85 (s, 1H), 5.36 (dd, $J = 3.6, 8.0$ Hz, 1H), 3.99 (s, 3H), 3.94 (s, 3H), 3.88 (s, 2H), 2.74-2.67 (m, 2H), 2.66 (s, 6H), 2.65-2.58 (m, 2H), 2.04-1.98 (m, 1H), 1.72-1.60 (m, 3H), 1.48-1.42 (m, 2H), 1.37-1.25 (m, 4H), 1.15 (t, $J = 6.8$ Hz, 3H); ^{13}C NMR (150 MHz, CDCl_3) δ 170.9, 154.7, 153.2, 150.3, 144.6, 138.1, 130.7, 128.2, 123.6, 119.3, 117.9, 106.0, 103.1, 80.7, 56.4, 56.2, 52.7, 51.8, 47.2, 45.3 (2C), 34.6, 29.0, 26.9, 25.6, 24.6, 10.6. HR-ESI-MS: Calcd. for $\text{C}_{27}\text{H}_{39}\text{N}_2\text{O}_4$ $[\text{M}+\text{H}]^+$: 455.2910, found: 455.2906.

4.2. Biological activity

4.2.1. Inhibition of AChE and BuChE

AChE from *Electrophorus electricus* (*EeAChE*, Sigma-Aldrich Co.) and BuChE from rat serum (*RatBuChE*) were used to determine the inhibitory activities of all the compounds according to the modified Ellman's method.³³ For *EeAChE* inhibition assay, 5,5'-dithiobis-2-nitrobenzoic acid (DTNB, 0.2%, 30 μL) (J&K Scientific) was added in a mixture of acetylthiocholine iodide (ATCI, 1 mM, 30 μL) (J&K Scientific), phosphate buffer solution (0.1 mM, pH = 8.0, 40 μL), different concentrations of test compounds (20 μL) and *EeAChE* (0.05 U/mL, final concentration, 10 μL), and then incubated at 37 °C for 15 min. The absorbance was measured at 412 nm by using a Varioskan Flash Multimode Reader (Thermo Scientific). For BuChE inhibition assay, 25% rat serum (10 μL) and S-butylthiocholine iodide (BTCl, 1 mM, 30 μL) (TCI Shanghai Development) were used and the assay was performed in a phosphate buffer (0.1 mM, pH = 7.4). Changes in absorbance were detected at 405 nm.^{23,45} The other procedure was similar with the method of *EeAChE* inhibition assay described above. IC_{50} values were calculated as the concentration of compound that produced 50% enzyme activity inhibition. Results are expressed as the mean \pm SD of at least three different experiments performed in triplicate.

4.2.2. Molecular Docking of AChE.

Molecular docking study of compounds **I-8**, **I-9**, **II-9** and **II-10** with *Torpedo californica* (*Tc*) AChE (PDB: *IEVE*) was performed using AUTODOCK 4.2 program. The crystal structure was downloaded from the Protein Data Bank. The 3D structure of these compounds and co-crystal ligand Donepezil was built and optimized by molecular mechanics, and then prepared by removing the hydrogen atoms, adding Gasteiger charges and their atomic charges to skeleton atoms, assigning the proper atomic types. By using Autodock Tools (ADT; version 1.5.6), water molecules and original inhibitor was removed, polar hydrogen atoms were added to amino acid residues and Gasteiger charges

were assigned to all atoms of AChE. The resulting enzyme structure was used as an input for the AUTOGRID program. All maps were calculated with 0.375 Å spacing between grid points. The center of the grid box was generated around the center of Donepezil with coordinates $x = 2.023$, $y = 63.295$, $z = 67.062$. The dimension of the active site box was set at $60 \times 60 \times 60$ Å. Other than the referred parameters above, the other parameters were used as default. Flexible ligand docking was used for the docking analyses. For the validation of the docking parameters, the co-crystal ligand was re-docked at the catalytic site of the protein. Each docking system was derived from 100 runs of the AUTODOCK using the Lamarckian genetic algorithm (LGA). Finally, a cluster analysis was performed on the docking results using a root mean square (RMS) tolerance of 1.0. Graphic manipulations and visualizations were conducted by Autodock Tools or Discovery Studio 2.5 software. The ligand interaction tool was used to view the interaction diagram of the ligands with the residues at the active site of AChE.

4.2.3. Antioxidant activity assay

The antioxidant activity of these compounds was determined by the oxygen radical absorbance capacity-fluorescein (ORAC-FL) assay.^{23,35} 2,2'-Azobis(amidinopropane) dihydrochloride (AAPH) was purchased from Accela ChemBio Co. Ltd. Fluorescein (FL) and 6-hydroxy-2,5,7,8-tetramethylchromane-2-carboxylic acid (Trolox) were purchased from TCI (Shanghai) Development. All the assays were performed in 75 mM phosphate buffer (pH = 7.4). Trolox was used as a standard (1-8 µM, final concentration). A blank (FL + AAPH) using phosphate buffer instead of antioxidant calibration were carried out in each assay. The samples were measured at 5 µM. A mixture of the tested compound (20 µL) and FL (120 µL, 150 nM final concentration) was placed in a black 96-well plate and pre-incubated for 15 min at 37 °C, followed by the addition of AAPH solution (60 µL, 12 mM final concentration) rapidly using an autosampler. The plate was immediately placed in a Varioskan Flash Multimode Reader (Thermo Scientific), and the fluorescence was recorded every minute for 90 min with excitation at 485 nm and emission at 535 nm. All reaction mixtures were prepared in triplicate, and at least three independent assays were performed for each sample. Antioxidant curves (fluorescence vs time) were normalized to the curve of the blank, and the area under the fluorescence decay curve (AUC) was calculated. The net AUC was obtained by subtracting the AUC of the blank. Regression equations between net AUC and Trolox concentrations were calculated. ORAC-FL values were expressed as Trolox equivalents by using the standard curve calculated for each sample, where

the ORAC-FL value of Trolox was taken as 1.0.

4.2.4. Inhibition of self-induced $A\beta_{1-42}$ aggregation

To investigate the self-induced $A\beta_{1-42}$ aggregation, a Thioflavin T-based fluorometric assay was performed.^{37,46} $A\beta_{1-42}$ was purchased from ChinaPeptides Co., Ltd. Thioflavin T (Basic Yellow 1, ThT) was purchased from TCI (Shanghai) Development. Hexafluoro-2-propanol (HFIP) was purchased from Energy Chemical. $A\beta_{1-42}$ was dissolved in HFIP (1 mg/mL) and incubated for 24 h at room temperature. Upon the solvent was evaporated, HFIP pretreated $A\beta_{1-42}$ was dissolved in dry DMSO to obtain a stable stock solution with a concentration of 200 μ M, which was stored at -80 °C until use. Solutions of test compounds were prepared in DMSO in 2.5 mM and diluted with phosphate buffer solution (pH = 7.4). A mixture of the $A\beta_{1-42}$ (20 μ L, 25 μ M) with the tested compounds (20 μ L, 25 μ M) was incubated at 37 °C for 24 h. After incubation, 160 μ L of 5 μ M ThT in 50 mM glycine-NaOH buffer (pH = 8.5) was added. Fluorescence was measured on a Varioskan Flash Multimode Reader (Thermo Scientific) with excitation and emission wavelengths at 446 nm and 490 nm, respectively. The fluorescence intensities were calculated after subtraction of the background activity. The percentage of inhibition was calculated by the expression $(1-IF_i/IF_c) \times 100$, in which IF_i and IF_c were the fluorescence intensities obtained for $A\beta_{1-42}$ in the presence and in the absence of inhibitors after subtracting the background fluorescence, respectively. Each measurement was run in triplicate.

4.2.5. Inhibition of MAOs

Recombinant human MAO-A and MAO-B were purchased from Sigma-Aldrich and stored at -80 °C. Potassium phosphate buffer (100 mM, pH = 7.4, containing 20.2 mM KCl) to a final volume of 500 μ L including kynuramine (45 μ M for MAO-A and 30 μ M for MAO-B) and various concentrations of test compounds (0-100 μ M) with the concentration of DMSO lower than 4% was required in the entire enzymatic reactions. Reactions were started by adding MAO-A or MAO-B (7.5 μ g/mL), and then the solutions were incubated for 30 min at 37 °C. After this incubation period, the reactions were finished by the addition of 400 μ L NaOH (2.0 mol/L) and 1000 μ L water, then centrifuged for 10 min. A Varioskan Flash Multimode Reader (Thermo Scientific) was used to determine the activity by measuring the fluorescence of the supernatant with excitation at 310 nm and emission at 400 nm.^{38,47} IC_{50} values were calculated from sigmoidal dose-response curves (graphs of the initial rate of kynuramine oxidation versus the logarithm of inhibitor concentration). Each sigmoidal curve was obtained from six different compound concentrations spanning at least three orders of magnitude. Data

analyses were performed with GraphPad Prism 5 employing the one site competition model. IC_{50} values were determined in triplicate and expressed as mean \pm SD.

4.2.6. *In vitro* blood-brain barrier permeation assay

The BBB permeability of the compounds was evaluated using a parallel artificial membrane permeation assay (PAMPA-BBB), in a similar manner as described previously.^{23,41} Commercial drugs were purchased from Sigma and Alfa Aesar. Porcine brain lipid (PBL) was purchased from Avanti Polar Lipids. The donor plate (MATRNPS50) and the acceptor plate (PVDF membrane, pore size 0.45 μ m, MAIPN4550) were obtained from Millipore. Filter PDVF membrane units (diameter 25 mm, pore size 0.45 μ m) from Pall Corporation were used to filter the samples. Compounds were dissolved in DMSO at 5 mg/mL and then diluted to 100 μ g/mL with PBS/EtOH (70:30). The filter membrane was impregnated with 4 μ L PBL in dodecane (20 μ g/mL) and the acceptor wells were filled with 200 μ L of PBS/EtOH (70:30). Then, 350 μ L of compound solutions (100 μ g/mL) was added to the donor wells. The acceptor filter plate was carefully put on the donor plate to form a sandwich, which was left undisturbed for 18 h at 25 °C. After incubation, the donor plate was separated and the concentration of compounds in the acceptor wells was determined by Varioskan Flash Multimode Reader (Thermo Scientific). Every sample was analyzed at ten wavelengths in four wells, and the results are given as the mean \pm SD from three independent runs. In the experiment, 11 quality control drugs with known BBB permeability were included to validate the analysis set. The assay validation was conducted by comparing the experimental permeability of commercial drugs with literature values, which gave a good linear correlation, $P_e(\text{exp.}) = 0.8792 \times P_e(\text{bibl.}) - 0.0616$ ($R^2 = 0.9555$).

4.2.7. Step-down passive avoidance test

4.2.7.1. Animals and treatment

Kunming mice at body weight of 18-22 g (male and female in half) were provided by the Center of Experimental Animals of Sichuan Academy of Chinese Medicine Sciences (eligibility certification no. SCXK-Sichuan 2013-19). The animals were housed in random groups of six per cage, with food and water available ad libitum. Mice were kept at a temperature of 24 ± 2 °C and a relative humidity of 50-60%, and under a 12-h light-dark cycle. All mice were given a commercial chow diet and allowed to adapt to the laboratory environment for at least 1 week before the experiments.

Animals were randomly distributed into six groups: a control group, a model group, a positive control group (5.0 mg/kg Donepezil, Eisai China Inc.), and three groups that received different doses

of compound **I-8** (1.0, 5.0, 25.0 mg/kg). Each group contained eight mice. The mice of positive control group and compound **I-8** groups were given Donepezil and **I-8** by intragastric administration (*i.g.*), once a day for 7 consecutive days. Control and model group were administered with an equal volume of 0.5% CMC-Na solution at the same time. The mice were submitted to behavioral tests one day after 7 days of treatment with compounds.

4.2.7.2. Assay method

The step-down passive avoidance test was used to assess the learning and memory capacity in mice.^{22,42} The apparatus consisted of a grid floor with a small platform in the center. The platform served as a shock free zone. The mice underwent two separate trials: a training trial and a test trial 24 h later. On day 6, training trial was conducted 1 h after administration. Mice were initially placed on the platform and given an electrical foot shock (50 V, 5 s) when the mouse stepped down on the grid floor. The training trial of each mouse was conducted for 5 min, and the first time to step down was recorded as latency time for learning performance. 30 min after the training test completion, memory impairment was induced by administering scopolamine (2.0 mg/kg, *i.p.*, J&K Scientific) to each group except for the control group. 24 h after the training trial, mice were placed again on the platform, the latency time and the number of shocks received within 5 min for test trial was measured.

4.2.8 Statistical analysis

Results are expressed as the mean \pm SEM. Statistical analysis of multiple groups was performed using one-way analysis of variance (ANOVA) with Student's *t* test in Prism (GraphPad, San Diego, CA, USA). In all cases, $p < 0.05$ was considered to be statistically significant.

Declaration of competing interests

The authors declare that they have no competing interests.

Acknowledgements

This work was supported by Sichuan Science and Technology Program (2018SZ0014, 2019YFS0088) and the Fundamental Research Funds for the Central Universities.

Supplementary data

The supplementary data associated with this article can be found in the online version.

References

1. Tang, H.; Zhao, H. T.; Zhong, S. M.; Wang, Z. Y.; Chen, Z. F.; Liang, H. Novel oxoisoaporphine-based inhibitors of acetyl- and butyrylcholinesterase and acetylcholinesterase- induced beta-amyloid aggregation. *Bioorg. Med. Chem. Lett.* **2012**, *22*, 2257.
2. Scarpini, E.; Scheltens, P.; Feldman, H. Treatment of Alzheimer's disease: current status and new perspectives. *Lancet Neurol.* **2003**, *2*, 539.
3. Bolognesi, M. L.; Cavalli, A.; Valgimigli, L.; Bartolini, M.; Rosini, M.; Andrisano, V.; Recanatini, M.; Melchiorre, C. Multi-target-directed drug design strategy: from a dual binding site acetylcholinesterase inhibitor to a trifunctional compound against Alzheimer's disease. *J. Med. Chem.* **2007**, *50*, 6446.
4. Querfurth, H. W.; LaFerla, F. M. Alzheimer's disease. *N. Engl. J. Med.* **2010**, *362*, 329.
5. Liston, D. R.; Nielsen, J. A.; Villalobos, A.; Chapin, D.; Jones, S. B.; Hubbard, S. T.; Shalaby, I. A.; Ramirez, A.; Nason, D.; White, W. F. Pharmacology of selective acetylcholinesterase inhibitors: implications for use in Alzheimer's disease. *Eur. J. Pharmacol.* **2004**, *486*, 9.
6. Reyes, A. E.; Chacón, M. A.; Dinamarca, M. C.; Cerpa, W.; Morgan, C.; Inestrosa, N. C. Acetylcholinesterase-A β complexes are more toxic than A β fibrils in rat hippocampus: effect on rat beta-amyloid aggregation, laminin expression, reactive astrocytosis, and neuronal cell loss. *Am. J. Pathol.* **2004**, *164*, 2163.
7. Hardy, J.; Selkoe, D. J. The amyloid hypothesis of Alzheimer's disease: progress and problems on the road to therapeutics. *Science.* **2002**, *297*, 353.
8. Jiang, C. S.; Fu, Y.; Zhang, L.; Gong, J. X.; Wang, Z. Z.; Xiao, W.; Zhang, H. Y.; Guo, Y. W. Synthesis and biological evaluation of novel marine-derived indole-based 1,2,4-oxadiazoles derivatives as multifunctional neuroprotective agents. *Bioorg. Med. Chem. Lett.* **2015**, *25*, 216.
9. Young, K. J.; Bennett, J. P. The mitochondrial secret(ase) of Alzheimer's disease. *J. Alzheimers Dis.* **2010**, *20*, 381.
10. Patil, P. O.; Bari, S. B.; Firke, S. D.; Deshmukh, P. K.; Donda, S. T.; Patil, D. A. A comprehensive review on synthesis and designing aspects of coumarin derivatives as monoamine oxidase inhibitors for depression and Alzheimer's disease. *Bioorg. Med. Chem.* **2013**, *21*, 2434.
11. Ma, J.; Yoshimura, M.; Yamashita, E.; Nakagawa, A.; Ito, A.; Tsukihara, T. Structure of rat

- monoamine oxidase A and its specific recognitions for substrates and inhibitors. *J. Mol. Biol.* **2004**, *338*, 103.
12. Bolea, I.; Juárez-Jiménez, J.; de los Ríos, C.; Chioua, M.; Pouplana, R.; Luque, F. J.; Unzeta, M.; Marco-Contelles, J.; Samadi, A. Synthesis, biological evaluation, and molecular modeling of donepezil and N-[(5-(benzyloxy)-1-methyl-1H-indol-2-yl)methyl]-N-methylprop-2-yn-1-amine hybrids as new multipotent cholinesterase/monoamine oxidase inhibitors for the treatment of Alzheimer's disease. *J Med Chem.* **2011**, *54*, 8251.
13. Ibrahim, M. M.; Gabr, M. T. Multitarget therapeutic strategies for Alzheimer's disease. *Neural Regen Res.* **2019**, *14*, 437.
14. Xu, J.; Wang, Y.; Li, N.; Xu, L.; Yang, H.; Yang, Z. L-3-n-butylphthalide improves cognitive deficits in rats with chronic cerebral ischemia. *Neuropharmacology.* **2012**, *62*, 2424.
15. Wang, Y. G.; Li, Y.; Wang, C. Y.; Ai, J. W.; Dong, X. Y.; Huang, H. Y.; Feng, Z. Y.; Pan, Y. M.; Lin, Y.; Wang, B. X.; Yao, L. L. L-3-n-Butylphthalide protects rats' cardiomyocytes from ischaemia/reperfusion-induced apoptosis by affecting the mitochondrial apoptosis pathway. *Acta Physiol.* **2014**, *210*, 524.
16. Yang, X. D.; Cen, Z. D.; Cheng, H. P.; Shi, K.; Bai, J.; Xie, F.; Wu, H. W.; Li, B. B.; Luo, W. L-3-n-Butylphthalide protects HSPB8 K141N mutation-induced oxidative stress by modulating the mitochondrial apoptotic and Nrf2 pathways. *Front. Neurosci.* **2017**, *11*, 402.
17. Peng, Y.; Xing, C.; Xu, S.; Lemere, C. A.; Chen, G.; Liu, B.; Wang, L.; Feng, Y.; Wang, X. L-3-n-butylphthalide improves cognitive impairment induced by intracerebroventricular infusion of amyloid-beta peptide in rats. *Eur. J. Pharmacol.* **2009**, *621*, 38.
18. Wang, C. Y.; Wang, Z. Y.; Xie, J. W.; Wang, T.; Wang, X.; Xu, Y.; Cai, J. H. DL-3-n-butylphthalide-induced upregulation of antioxidant defense is involved in the enhancement of cross talk between CREB and Nrf2 in an Alzheimer's disease mouse model. *Neurobiol. Aging.* **2016**, *38*, 32.
19. Qi, Q.; Xu, J.; Lv, P.; Dong, Y.; Liu, Z.; Hu, M.; Xiao, Y.; Jia, W.; Jin, W.; Fan, M.; Zhang, D.; Meng, N. DL-3-n-butylphthalide alleviates vascular cognitive impairment induced by chronic cerebral hypoperfusion by activating the Akt/Nrf2 signaling pathway in the hippocampus of rats. *Neurosci. Lett.* **2018**, *672*, 59.
20. Huang, J. Z.; Chen, Y. Z.; Su, M.; Zheng, H. F.; Yang, Y. P.; Chen, J.; Liu, C. F. dl-3-n-

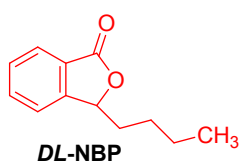
Butylphthalide prevents oxidative damage and reduces mitochondrial dysfunction in an MPP(+)-induced cellular model of Parkinson's disease. *Neurosci. Lett.* **2010**, *475*, 89.

21. Kryger, G.; Silman, I.; Sussman, J. L. Structure of acetylcholinesterase complexed with E2020 (Aricept): implications for the design of new anti-Alzheimer drugs. *Structure.* **1999**, *7*, 297.
22. Qiang, X. M.; Sang, Z. P.; Yuan, W.; Li, Y.; Liu, Q.; Bai, P.; Shi, Y. K.; Tan, Z. H.; Deng, Y. Design, synthesis and evaluation of genistein-O-alkylbenzylamines as potential multifunctional agents for the treatment of Alzheimer's disease. *Eur. J. Med. Chem.* **2014**, *76*, 314.
23. Luo, L.; Li, Y.; Qiang, X. M.; Cao, Z. C.; Xu, R.; Yang, X.; Xiao, G. Y.; Song, Q.; Tan, Z. H.; Deng, Y. Multifunctional thioxanthone derivatives with acetylcholinesterase, monoamine oxidases and β -amyloid aggregation inhibitory activities as potential agents against Alzheimer's disease. *Bioorg. Med. Chem.* **2017**, *25*, 1997.
24. Riches, S. L.; Saha, C.; Filgueira, N. F.; Grange, E.; McGarrigle, E. M.; Aggarwal, V. K. On the mechanism of ylide-mediated cyclopropanations: evidence for a proton-transfer step and its effect on stereoselectivity. *J. Am. Chem. Soc.* **2010**, *132*, 7626.
25. Parikh, J. R.; Doering, W. E. Sulfur trioxide in the oxidation of alcohols by dimethyl sulfoxide. *J. Am. Chem. Soc.* **1967**, *89*, 5505.
26. Jiang, B.; Shi, D. Y.; Cui, Y. C.; Guo, S. J. Design, synthesis, and biological evaluation of bromophenol derivatives as protein tyrosine phosphatase 1B inhibitors. *Arch. Pharm.* **2012**, *345*, 444.
27. Beck, D. E.; Agama, K.; Marchand, C.; Chergui, A.; Pommier, Y.; Cushman, M. Synthesis and biological evaluation of new carbohydrate-substituted indenoisoquinoline topoisomerase I inhibitors and improved syntheses of the experimental anticancer agents indotecan (LMP400) and indimitecan (LMP776). *J. Med. Chem.* **2014**, *57*, 1495.
28. Napoletano, M.; Norcini, G.; Pellacini, F.; Marchini, F.; Morazzoni, G.; Ferlenga, P.; Pradella, L. Phthalazine PDE4 inhibitors. Part 2: the synthesis and biological evaluation of 6-methoxy-1,4-disubstituted derivatives. *Bioorg. Med. Chem. Lett.* **2001**, *11*, 33.
29. Boussard, M. F.; Truche, S.; Rousseau-Rojas, A.; Briss, S.; Descamps, S.; Droual, M.; Wierzbicki, M.; Ferry, G.; Audinot, V.; Delagrangue, P. New ligands at the melatonin binding site MT(3). *Eur. J. Med. Chem.* **2006**, *41*, 306.
30. Harig, M.; Neumann, B.; Stammer, H. G.; Kuck, D. 2,3,6,7,10,11-hexamethoxy

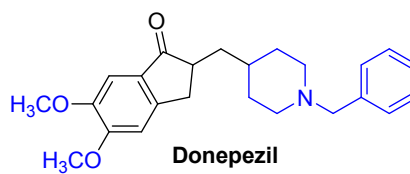
- tribenzotriquinacene synthesis, solid-state structure, and functionalization of a rigid analogue of cyclotrimeratrylene. *Eur. J. Org. Chem.* **2004**, 2004, 2381.
31. Sevenard, D. V.; Sosnovskikh, V. Y.; Schroeder, G.; Rösenthaller, G. V. 3-Polyfluoroacrylmethylene phthalides: synthesis and structure. *Aust. J. Chem.* **2001**, 54, 335.
32. Watanabe, M.; Ijichi S.; Morimoto, H.; Nogami, K.; Furukawa, S. Wittig-horner reaction of dimethyl phthalide-3-phosphonates with aldehydes: synthesis of 3-ylidenephthalides and characterization of their *E*- and *Z*-isomers. *Heterocycles* **1993**, 36, 553.
33. Li, Y.; Qiang, X. M.; Luo, L.; Li, Y. X.; Xiao, G. Y.; Tan, Z. H.; Deng, Y. Synthesis and evaluation of 4-hydroxyl aurone derivatives as multifunctional agents for the treatment of Alzheimer's disease. *Bioorg. Med. Chem.* **2016**, 24, 2342.
34. Najafi, Z.; Mahdavi, M.; Saeedi, M.; Karimpour-Razkenari, E.; Asatouri, R.; Vafadarnejad, F.; Moghadam, F. H.; Khanavi, M.; Sharifzadeh, M.; Akbarzadeh, T. Novel tacrine-1,2,3-triazole hybrids: In vitro, in vivo biological evaluation and docking study of cholinesterase inhibitors. *Eur. J. Med. Chem.* **2017**, 125, 1200.
35. Fang, L.; Kraus, B.; Lehmann, J.; Heilmann, J.; Zhang, Y. H.; Decker, M. Design and synthesis of tacrine-ferulic acid hybrids as multi-potent anti-Alzheimer drug candidates. *Bioorg. Med. Chem. Lett.* **2008**, 18, 2905.
36. García-Font, N.; Hayour, H.; Belfaitah, A.; Pedraz, J.; Moraleda, I.; Iriepa, I.; Bouraiou, A.; Chioua, M.; Marco-Contelles, J.; Oset-Gasque, M. J. Potent anticholinesterasic and neuroprotective pyranotacrines as inhibitors of beta-amyloid aggregation, oxidative stress and tau-phosphorylation for Alzheimer's disease. *Eur. J. Med. Chem.* **2016**, 118, 178.
37. Bartolini, M.; Bertucci, C.; Bolognesi, M. L.; Cavalli, A.; Melchiorre, C.; Andrisano, V. Insight into the kinetic of amyloid beta (1-42) peptide self-aggregation: elucidation of inhibitors' mechanism of action. *Chembiochem.* **2007**, 8, 2152.
38. Legoabe, L. J.; Petzer, A.; Petzer, J. P. Selected C7-substituted chromone derivatives as monoamine oxidase inhibitors. *Bioorg. Chem.* **2012**, 45, 1
39. <https://www.molinspiration.com/cgi-bin/properties>.
40. Romano, B.; Plano, D.; Encío, I.; Palop, J. A.; Sanmartín, C. In vitro radical scavenging and cytotoxic activities of novel hybrid selenocarbamates. *Bioorg. Med. Chem.* **2015**, 23, 1716.
41. Di, L.; Kerns, E. H.; Fan, K.; McConnell, O. J.; Carter, G. T. High throughput artificial membrane

- permeability assay for blood-brain barrier. *Eur. J. Med. Chem.* **2003**, *38*, 223.
42. Kwon, S.H.; Lee, H.K.; Kim, J. A.; Hong, S. I.; Kim, H. C.; Jo, T. H.; Park, Y. I.; Lee, C. K.; Kim, Y. B.; Lee, S.Y.; Jang, C. G. Neuroprotective effects of chlorogenic acid on scopolamine-induced amnesia via anti-acetylcholinesterase and antioxidative activities in mice, *Eur. J. Pharmacol.* **2010**, *649*, 210.
43. Kumpaty, H. J.; Williamson, J. S.; Bhattacharyya, S. Synthesis of *N*-methyl secondary amines. *Synth. Commun.* **2003**, *33*, 1411.
44. Bhattacharjee, D.; Popp, F. D. New compounds: reissert compound studies XXXII: facile synthesis of 3-azapapaverine. *J. Pharm. Sci-US.* **1980**, *69*, 120.
45. Lu, C. J.; Zhou, Q.; Yan, J.; Du, Z. Y.; Huang, L.; Li, X. S. A novel series of tacrine-selegiline hybrids with cholinesterase and monoamine oxidase inhibition activities for the treatment of Alzheimer's disease. *Eur. J. Med. Chem.* **2013**, *62*, 745.
46. Li, R. S.; Wang, X. B.; Hu, X. J.; Kong, L. Y. Design, synthesis and evaluation of flavonoid derivatives as potential multifunctional acetylcholinesterase inhibitors against Alzheimer's disease. *Bioorg. Med. Chem. Lett.* **2013**, *23*, 2636.
47. Strydom, B.; Malan, S. F.; Castagnoli, N.; Bergh, J. J.; Petzer, J. P. Inhibition of monoamine oxidase by 8-benzyloxycaffeine analogues. *Bioorg. Med. Chem.* **2010**, *18*, 1018.

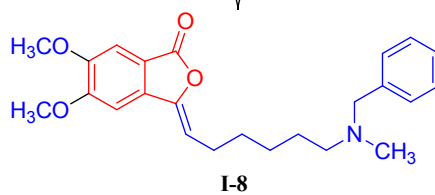
Graphical Abstract



EeAChE IC₅₀: no active
 ORAC-FL value: 0.21 Trolox equiv
 Self-induced A β ₄₂ aggregation: < 5.0 % at 25 μ M



EeAChE IC₅₀: 26.4 nM
RatBuChE IC₅₀: 44.6 μ M
 Self-induced A β ₄₂ aggregation: < 5.0 % at 25 μ M



EeAChE IC₅₀: 2.66 nM
RatBuChE: 19.10 % inhibition at 50 μ M
 ORAC-FL value: 0.40 Trolox equiv
 Self-induced A β ₁₋₄₂ aggregation: 19.45 % at 25 μ M
 Good BBB permeability *in vitro*
 Reversed scopolamine-induced memory deficit in mice

Highlights

- Phthalide alkyl tertiary amine derivatives were synthesized.
- Almost all compounds displayed significant AChE inhibitory and selective activities.
- Most compounds exhibited increased self-induced $A\beta_{1-42}$ aggregation inhibitory activity.
- Compound **I-8** displayed excellent BBB permeability *in vitro*.
- Compound **I-8** significantly reversed scopolamine-induced memory deficit in mice.